

Sense of Agency for intracortical brain machine interfaces

Andrea Serino^{*1,2}, Marcie Bockbrader^{*3}, Tommaso Berton¹, Sam Colachis^{3p,4c}, Marco Solca², Collin Dunlap^{3,4}, Kaitie Eipel^{3p}, Patrick Ganzer⁴, Nick Annetta⁴, Gaurav Sharma^{4p,9c}, Pavo Orepic², David Friedenberg⁴, Per Sederberg⁵, Nathan Faivre^{2,6}, Ali Reza^{**7}, Olaf Blanke^{**2,8}

¹MySpace Lab, Department of Clinical Neuroscience, University Hospital Lausanne (CHUV), Lausanne, Switzerland; ²Laboratory of Cognitive Neuroscience, Brain Mind Institute & Center for Neuroprosthetics, Ecole Polytechnique Fédérale de Lausanne (EPFL), Campus Biotech, Geneva, Switzerland; ³Department of Physical Medicine and Rehabilitation, The Ohio State University, Columbus, Ohio, US; ⁴Medical Devices and Neuromodulation, Battelle Memorial Institute, Columbus, Ohio, US; ⁵Department of Psychology, University of Virginia, Charlottesville, Virginia, US; ⁶Univ. Grenoble Alpes, Univ. Savoie Mont Blanc, CNRS, LPNC, 38000 Grenoble, France; ⁷Rockefeller Neuroscience Institute, West Virginia University, Morgantown, West Virginia, US; ⁸Department of Neurology, University Hospital, Geneva, Switzerland; ⁹Air Force Research Laboratory, Dayton, Ohio, US.

* These authors contributed equally; ** These authors jointly supervised this work.
^p prior affiliation at time of work; ^c current affiliation

* These authors contributed equally; ** These authors jointly supervised this work.

Corresponding authors:

Andrea Serino - andrea.serino@unil.ch

Olaf Blanke – olaf.blanke@epfl.ch

43 **Abstract**

44 Intracortical brain machine interfaces decode motor commands from neural signals and
45 translate them into actions, enabling movement for paralyzed individuals. The subjective
46 sense of agency associated to actions generated via intracortical brain machine
47 interfaces, the involved neural mechanisms and its clinical relevance are currently
48 unknown. By experimentally manipulating the coherence between decoded motor
49 commands and sensory feedback in a tetraplegic individual using a brain machine
50 interface, we provide evidence that primary motor cortex processes sensory feedback,
51 sensorimotor conflicts and subjective states of actions generated via the brain machine
52 interface. Neural signals processing the sense of agency affected the proficiency of the
53 brain machine interface, underlining the clinical potential of the present approach.
54 These findings show that primary motor cortex encodes information related to action
55 and sensing, but also sensorimotor and subjective agency signals, which in turn are
56 relevant for clinical applications of brain machine interfaces.

57
58
59
60
61
62
63
64
65
66
67
68
69
70
71
72
73
74

75 **Main text**

76

77 **Introduction**

78 When performing a voluntary movement, motor commands from the brain activate body
79 effectors, which produce a cascade of refferent sensory (proprioceptive, tactile, visual)
80 cues. Motor commands are also associated with prediction signals about the sensory
81 consequences of the movement. The congruency between motor commands, refferent
82 sensory feedback, and sensory predictions is at the basis of the sense of agency, our
83 feeling of being in control of our actions¹⁻³. In case of damage to the motor system,
84 motor commands that would trigger actions do not reach body effectors, leading to
85 different types of paralysis, depending on the location and severity of damage.
86 Intracortical brain machine interfaces (BMI) bypass such brain-body disconnection by
87 decoding brain signals from different regions (i.e., primary motor cortex (M1), parietal or
88 premotor cortex) and translating them into motor commands for the control of robots,
89 exoskeletons^{4,5}, neuromuscular functional electrical stimulation^{6,7} or other devices⁸,
90 enabling different actions (BMI actions) for patients with severe neuromotor
91 impairments⁹.

92

93 Here we study how it feels to generate movements with an intracortical-BMI, that is
94 what is the sense of agency for BMI actions ((see ^{10,11} for recent studies with non-
95 invasive brain computer interfaces (BCI)) and search for a potential neural mechanism.
96 In particular, we asked whether motor neurons in human M1 encode not only motor
97 commands, but also sensory feedback and whether these signals covary with agency
98 for BMI actions Finally we tested whether agency also affects the efficiency of the BMI
99 system - i.e. whether agency has a potential therapeutic benefit.

100

101 We applied classic approaches from psychophysics, neurophysiology,
102 neuroengineering and virtual reality (VR) to ask these questions in a patient suffering
103 from tetraplegia (caused by severe cervical spinal cord injury; C5/C6), who had been a
104 BMI expert for two years before the start of the present study⁶. The patient had no
105 preserved motor function below the C5 level. His sensory functions were extremely

106 limited and only showed partially preserved function at the C6 level on the left side and
107 at C5 on the right side (there was also residual sensation for pressure on his right
108 thumb). Concerning proprioception, he had preserved perception for shoulder, elbow
109 and wrist joint position, but no proprioception for digits joint position (see Material and
110 methods for more details).

111
112 The BMI consisted of a 96-channel array implanted in the hand area of left M1 and
113 actuated a transcutaneous forearm neuromuscular electrical stimulation (NMES) system
114 (see ⁶ for a full description of the system) to translate decoded cortical signals into right
115 forearm and hand movements. In order to study the sense of agency for BMI actions
116 and to evaluate its clinical impact, we experimentally manipulated the congruency
117 between the decoded actions and the actions actuated by the BMI-NMES system. As
118 illustrated in Figure 1, the participant was instructed to realize a cued action with the
119 BMI and was provided with movement-related sensory feedback using visual (via VR)
120 and/or somatosensory (via NMES) stimulation. Critically, this feedback was either
121 congruent or incongruent with respect to the motor commands decoded from M1: half of
122 the trials, in which the decoded action corresponded to the cued action (e.g., open
123 hand), were associated with congruent feedback (e.g., open hand), while the other half
124 were associated with incongruent feedback (e.g. the opposite action: close hand). For
125 each BMI action, we asked the participant whether he felt in control of that action and to
126 rate his confidence about this judgement, allowing us to (1) gauge the sense of agency
127 for BMI actions and how this was modulated by the congruency between motor
128 commands and sensory feedback. Next, neural data from the M1 implant were analyzed
129 to measure how (2) the sense of agency and (3) sensory feedback were encoded in the
130 activity of M1 neurons, quantified as multi-unit (MU) firing rates and local field potentials
131 (LFP). Finally, we investigated (4) how visual and somatosensory feedback, and the
132 associated sense of agency, affected the performance of the BMI system by changing
133 the pattern of response of M1 neurons. By investigating what it feels like to control
134 actions mediated by an intracortical BMI, our data show neural patterns in M1 activity
135 (MU and LFP) reflecting the processing of agency for BMI actions, as generated by the
136 congruency between intention and sensory feedback. Importantly, we show that the
137 nature of somatosensory feedback (and the related sense of agency) affected the

138 efficiency of the BMI system by modulating the response properties of M1 neurons,
139 underlining the clinical relevance of sensory feedback and agency for the BMI field.

140

141 During the experiment, the participant was cued to execute one of four target actions
142 (hand opening, hand closing, thumb extension, thumb flexion) using a validated BMI
143 neuroprosthesis. Neural activity corresponding to each target movement was recorded
144 via a 96-channel microelectrode array in M1 and a nonlinear support vector machine
145 classifier was applied to decode the participant's chosen action from MU activity (see ⁶
146 for full description). On each trial, the classifier provided the likelihood of each target
147 action (on a -1 to +1 range, in 100 ms bins), thus decoding one of the four target actions
148 from the participant's M1 activity. In three different experiments, visual, somatosensory,
149 or visual-somatosensory feedback about the BMI action was provided (Figure 1). In
150 Experiment 1, VR was used to provide visual feedback, consisting of a life-size virtual
151 arm on a monitor superimposed over the participant's right arm, matching the location
152 and dimensions of the participant's real arm, which was occluded from view. In
153 Experiment 2, NMES was used to provide 'somatosensory' feedback: the patient's
154 upper limb muscles were electrically stimulated so he could feel, but not see the
155 selected movement. Experiment 3 combined VR and NMES to provide 'visual-
156 somatosensory feedback' (see below). In half of the trials, sensory feedback was
157 congruent with the cued action, while in the other half it was incongruent (i.e., the
158 opposite, action was executed) (see Figure 1B). At the end of each trial, we gauged the
159 participant's sense of agency (0 or 1; Q1) and confidence (rating between 0 and 100;
160 Q2). Importantly, the amount of sensory information was kept constant across
161 experiments, by providing non-informative sensorimotor feedback in Experiment 1 (i.e.,
162 a pattern of NMES triggering no BMI action) and non-informative visual feedback in
163 Experiment 2 (i.e., a static visual hand performing no action).

164

165

166 **Results**

167 **Sensory feedback determines agency and confidence.** Agency ratings were
168 collected in a total of 844 trials (155, 243 and 448 trials for Experiments 1, 2 and 3,
169 respectively; for Experiment 3 see below and Supplementary Information) and

170 compared across feedback conditions using permutation tests. A null distribution of the
171 mean agency rating was created by shuffling the condition labels over 10'000 iterations.
172 P-values (2-sided) were estimated by counting the proportion of shuffled samples
173 exceeding the observed average difference across conditions. As expected, and as
174 shown in Figure 2A, we were able to manipulate agency and confidence for BMI
175 actions. Thus, congruent visual (Experiment 1, 93.8% (bootstrapped 95% confidence
176 interval 93.4% - 94.2%) and 5.2% (4.8% - 5.6%) of positive responses to Q1 for
177 congruent and incongruent trials, respectively, $p < .0001$) and congruent somatosensory
178 (Experiment 2, 97.5% (97.3% - 97.6%) and 8.8% (8.4% - 9.1%) of positive responses
179 for congruent and incongruent trials respectively, $p < .0001$) feedback resulted in more
180 frequent agency responses versus incongruent conditions. Analyzing the role of
181 feedback for confidence ratings (irrespective of the agency ratings), we found that
182 confidence was modulated by somatosensory congruency (Experiment 2, Q2 ratings
183 were higher for somatosensory congruent [M = 74.0 (73.9 - 74.2)] than incongruent [M =
184 65.0 (64.8 - 65.2)] feedback; $p < 0.001$). The effect of visual congruency on confidence
185 ratings was not significant (Experiment 1, mean Q2 rating = 70.9 (70.6 - 71.1) for
186 congruent, 73.4 (73.1 - 73.6) for incongruent trials; $p = 0.28$).

187
188 In order to disentangle the role of visual and somatosensory cues for agency and
189 confidence, Experiment 3 combined VR and NMES including combinations of congruent
190 and incongruent visual and somatosensory feedback (Figure 1). Most relevant are the
191 comparisons between feedback conditions in which visual (V) and somatosensory (S)
192 signals were both congruent (+) or both incongruent (-) (V+/S+; V-/S-) or when feedback
193 was congruent in one modality and incongruent in the other modality (V+/S-; V- /S+).
194 Results revealed that somatosensory congruency was more effective in driving the
195 sense of agency and the associated confidence: ratings were higher not only when both
196 feedback signals were congruent (Q1 = 100% "Yes", mean Q2 = 83.98 [83.7 - 84.0]) as
197 compared to both being incongruent (Q1 = 7.6% "Yes" [7.2% - 7.9%], mean Q2 = 72.4
198 [72.2 - 72.6]), both p -values < 0.001), but also in the V- /S+ (Q1 = 68.9% "Yes" [68.4% -
199 69.4%], mean Q2 = 59.4 [59.3 - 59.6] as compared to the V+/S- condition (Q1 = 52.2%
200 "Yes" [51.5% - 52.8%], mean Q2 = 54.6 [54.4 - 54.8]; $p = 0.0035$ and $p = 0.036$, for
201 agency and confidence respectively) (Figure 2). Collectively, these data from

202 Experiments 1-3 show that the congruency between decoded actions and sensory
203 feedback, especially for the somatosensory modality, alters the sense of agency and
204 confidence for actions mediated by an intracortical BMI.

205

206 The sense of agency has been traditionally studied by presenting participants with
207 different visuo-motor couplings^{2,12-15}. In comparison, the role of somatosensory signals
208 remains poorly understood¹⁶, notably because it is normally impossible to decouple
209 motor commands, somatosensory feedback and visual feedback, with extremely rare
210 exceptions as in deafferented patients. Here we were able to contrast feedback cues
211 that were congruent in one modality (e.g., visual) and incongruent in the other modality
212 (e.g., somatosensory; and vice versa) with respect to the motor command and
213 demonstrate that somatosensory cues dominate the sense of agency and the
214 associated confidence for BMI-NMES actions. Of note, this effect cannot be due to the
215 presence of somatosensory cues alone, as BMI actions in the visual condition were
216 always associated with non-informative NMES stimulation producing somatosensory
217 sensations without generating any actions (i.e., pseudo random somatosensory
218 feedback, see Supplementary Information). Collectively these psychophysical data in a
219 BMI expert reveal that agency for BMI actions depends on visual and somatosensory
220 feedback (tactile and proprioceptive input) with somatosensory cues being more
221 relevant.

222

223 **Cortical signatures of sensory feedback in M1.** We next investigated how such
224 sensory feedback, that modulated the sense of agency, was encoded in M1 activity. We
225 first analyzed the LFP amplitude in the different feedback conditions across the three
226 experiments, using a regularized generalized linear model (ridge regression) and input
227 signals from each individual channel at every time point (see Supplementary
228 Information). As shown in Figure 3A (left), the analysis distinguished congruent vs.
229 incongruent visual feedback (maximum Cohen's Kappa $K = 0.40$, $t\text{-sum} = 219.4$, $p <$
230 0.001) within a single period of a positive potential that lasted from $\sim 700\text{-}1200$ ms after
231 the BMI action classification onset (Experiment 1). We could also distinguish congruent
232 vs. incongruent somatosensory feedback (maximum Cohen's Kappa $K = 0.64$, $t\text{-sum} =$
233 979.8 , $p < 0.001$) during two time periods: an early period characterized by a negative

234 potential (stronger for incongruent feedback), starting at ~200 ms after BMI
235 classification onset, followed by a later persistent differentiation lasting almost until the
236 end of the trial. These results were further corroborated by data from Experiment 3:
237 congruent trials in both modalities were clearly distinguished from incongruent trials in
238 both modalities, lasting from ~250-1900 ms after BMI classification onset (maximum $K =$
239 0.66 , $t\text{-sum} = 958.8$, $p < 0.001$). In addition, $V+/S-$ trials were different from $V-/S+$ trials
240 from ~300-1400 ms from BMI classification onset (maximum $K = 0.31$, $t\text{-sum} = 256.7$, p
241 < 0.001) (Figure 3B left). These findings show that visual and somatosensory feedback
242 were both encoded by LFPs in human M1 and that such M1-LFP coding started earlier
243 and was more stable over time for somatosensory feedback.

244

245 Applying the same decoding algorithm as for LFPs, we next determined if sensory
246 feedback was also encoded by the spiking rate of MU in M1 (for methods see
247 Supplementary Information). As shown in Figure 3A (right), in Experiment 1, MU activity
248 distinguished between congruent and incongruent visual feedback from ~400-900 ms
249 from BMI classification onset (max K value = 0.41 , $t\text{-sum} = 56.2$, $p < .001$). Extending
250 LFP findings, an earlier and more stable differentiation between congruent and
251 incongruent somatosensory feedback was found in MU activity in Experiment 2, with an
252 effect as early as ~200 ms from the BMI classification onset (max K value = 0.66 , $t\text{-sum}$
253 $= 390.7$, $p = < .001$) and then persisted from 800 to 2000 ms. Similar results were found
254 in Experiment 3 (Figure 3B, right), where MU activity distinguished between trials
255 congruent and incongruent in both modalities (max K value = 0.68 , $t\text{-sum} = 271.8$, $p = <$
256 $.001$) and between $V+/S-$ and $V-/S+$ trials from ~160 ms from BMI classification onset
257 (max K value = 0.55 , $t\text{-sum} = 151.2$, $p = < .001$). These data show that LFP and MU
258 activity reflects visual and somatosensory feedback during actions driven by a BMI
259 neuroprosthesis, with M1 activity early reflecting somatosensory feedback starting ~200
260 ms after NMES activation (~150 ms after BMI classification onset, ~200 ms before M1
261 activity encoding visual feedback) and persisting for a longer period.

262

263 The role of somatosensory and visual information is an important topic in motor control,
264 with robust evidence showing how perturbations of sensory feedback impact motor

265 execution and adaptation¹⁷. The present data show that the congruency between an
266 intended action and somatosensory/visual feedback is encoded by M1 neurons at
267 different latencies. Previous studies in non-human primates described responses in M1
268 related to tactile and visual input^{18,19}, during active and passive movements²⁰ and during
269 visual feedback of a pre-recorded movement^{21,22}. The present results are consistent
270 with proposals that suggest that M1 activity codes both for movement types and their
271 sensory consequences, in line with recent works describing how M1 neurons encode
272 different movement parameters (see ^{19,23,24} for reviews). Here we report that, at the
273 population level, human M1 activity in addition discriminates between arm movements
274 that were congruent or incongruent with the motor command, as defined by
275 somatosensory and visual feedback, with higher accuracy, earlier and more consistent
276 processing for the former type of sensory information. Thus, neural coding in M1
277 contains, at the population level, information not only about the movement itself, but
278 also about sensory consequences of actions, involving somatosensory-motor and visuo-
279 motor loops. These results are important to explain how sensory feedback affects the
280 proficiency of the BMI system as described below.

281

282 **Cortical signatures of the sense of agency in M1.** It is known that sensory-motor
283 congruency is a key mechanism of agency for able-bodied actions^{2,3}; here we have
284 shown that this also applies to agency and confidence for BMI-mediated actions and
285 that LFPs and MU activity in human M1 distinguishes congruent vs. incongruent BMI
286 actions. Next, we investigated to what extent LFP and MU activity in M1 also
287 discriminate actions with and without an accompanying sense of agency. For each trial,
288 we sorted LFP responses as a function of whether the participant reported agency or
289 not. As seen in Figure 4A (left), LFP activity starting ~270 ms after BMI classification
290 onset was found to code for agency and reached a maximum information value (Max K
291 = 0.41, t-sum = 1258.3, p < 0.001) at ~1000 ms after BMI movement onset. Thus, BMI
292 actions for which the participant felt to be the agent were characterized by a different
293 LFP pattern compared to BMI actions for which he did not. This was corroborated by
294 MU activity analysis (Figure 4A, right). The MU firing rate was higher for trials with
295 versus no agency; this discrimination started at ~300ms after BMI classification onset,

296 until 500 ms, and peaked at ~400 ms (max K = 0.45, t-sum = 232.5, p < 0.001). Later
297 on, MU activity also differentiated for agency, with higher firing rate for trials with no
298 agency (800-1600 ms after BMI classification). The same decoding was also able to
299 discriminate trials with high vs. low confidence, based on a median split of Q2, from
300 LFPs (max K = 0.296 at ~1200 ms, t-sum = 8449.3, p < 0.001) and MU (max K = 0.225
301 at ~400 ms, t-sum = 214.9, p < 0.001).

302

303 In the experimental design, sensory feedback congruency was used to modulate the
304 sense of agency and this may have influenced these agency findings. Accordingly, we
305 next tested whether LFP and MU contained information related to the sense of agency
306 per se, after controlling for the effect of sensory feedback. For this we built a continuous
307 measure of sense of agency and confidence allowing us to regress out the effect of
308 sensory feedback. This new index was computed by recoding confidence ratings (Q2)
309 as -Q2, for trials with no agency (as indicated in Q1) and +Q2 for trials with agency
310 (from Q1). This index was then orthogonalized with respect to congruency in order to
311 regress out this effect from the agency scores. As M1 signals also varied as a function
312 of the different cued actions (see SI), the index was also orthogonalized for the type of
313 action. We then used the same decoder to predict orthogonalized agency scores from
314 LFP and MU activity over time. This analysis shows that LFPs predicted the sense of
315 agency starting at ~450 ms after BMI classification onset (max $R^2 = 0.03$, t-sum = 69.8,
316 p = 0.017) (see Figure 4B left). A similar pattern was found when considering MU
317 activity, although the peak failed to reach significance after cluster-based correction for
318 multiple comparisons (Figure 4B right). These data show that M1 activity encodes the
319 sense of agency and associated confidence level and was modulated by the
320 congruency between motor commands and sensory feedback. Thus, subjective mental
321 states associated with BMI actions and control are encoded by M1 activity at the LFP
322 level (and to a minor extent at MU), independent of the neural processing associated
323 with sensory feedback (see Supplementary Information for single channel analyses).

324

325 **Somatosensory feedback modulates BMI classifier accuracy.** Given the strong role
326 of sensory congruency in determining agency and its coding in M1, we finally asked

327 whether sensory feedback has any impact on the BMI classifier. To this aim, we tested
328 whether the congruency between the decoded motor commands and sensory feedback
329 (visual, somatosensory) affected the accuracy of the BMI classifier, defined as the
330 summed suprathreshold activation values across a 4s window. In Experiments 1 and 2
331 we found that congruent somatosensory feedback improved classifier accuracy ($t(241)$
332 $= 9.29$, Cohen's $d = 1.238$, $p < 0.001$) (Figure 5B right). There was no effect due to
333 visual feedback ($t(153) = 1.523$, Cohen's $d = -0.245$, $p = 0.14$) (Figure 5A). Moreover,
334 incongruent somatosensory feedback was associated with lower classifier accuracy for
335 the cued movement (Figure 5B left), and even increased classifier accuracy for the
336 opposite movement (Figure 5B left). Thus, only somatosensory feedback congruency
337 affected BMI accuracy in the present participant. This was extended by the results of
338 Experiment 3, where we found a significant main effect of sensory feedback condition
339 ($F(3,444) = 15.83$, $\eta^2 = 0.097$, $p < 0.001$; Figure 5C). Further post-hoc corrected tests
340 showed that the BMI classifier's accuracy was higher when feedback was congruent,
341 than incongruent, in either modality (Tukey corrected $t = 4.966$, Cohen's $d = 0.666$, $p <$
342 0.001). More interestingly, when feedback was congruent for the somatosensory
343 modality and incongruent for the visual modality (V-/S+) BMI accuracy was higher than
344 in the opposite feedback condition (S-/V+) ($t = 4.558$, Cohen's $d = 0.612$, $p < 0.001$).
345 Figure 5 also shows the modulation of the BMI decoder as function of sensory feedback
346 over time during the trial. Significant change of the decoder's output is visible from 430
347 ms from somatosensory feedback.

348 These data from Experiments 1-3 show that BMI performance is affected by the
349 congruency between the decoded motor commands and the somatosensory feedback
350 induced by the action actuated by NMES. This finding is also coherent with the more
351 reliable (i.e., earlier, more long-lasting and better decoded) processing of
352 somatosensory feedback from M1 activity (LFP, MU). The fact that the same action as
353 actuated by NMES (e.g., open hand) increased or decreased the BMI classifier
354 performance, depending on whether somatosensory feedback was congruent (open
355 hand) or incongruent (close hand) with the cued action, excludes that this effect was a
356 generic artifact of NMES stimulation affecting the input to the BMI classifier
357 independently from sensory information.

358 In order to better understand how somatosensory feedback affected the accuracy of the
359 BMI classifier, we analyzed time point by time point changes in multiunit activity for the
360 whole array. We computed the average Euclidean distance between firing patterns of
361 trials with a given cued movement and either congruent or incongruent somatosensory
362 feedback. For a given cued movement (e.g., movement hand open) at congruent
363 feedback (hand open), we computed its distance either with the same movement (cued:
364 hand open) at incongruent feedback (hand close) or with the opposite movement (hand
365 close), at its relative incongruent feedback (hand open). This way, we compared cases
366 with the same motor intention, but opposite sensory feedback, and trials with the
367 opposite motor intention, but the same sensory feedback. As shown in Figure 6, trials
368 from Experiment 2 with opposite somatosensory feedback, but the same motor
369 intention, diverge after sensory feedback, whereas trials with opposite motor intention,
370 but the same sensory feedback, seem to even converge slightly with respect to
371 baseline. This shows that M1 activity after feedback reflects the movement implemented
372 via NMES more than the intended movement, thus explaining the modulation of
373 somatosensory feedback in BMI proficiency (see Figure 6B). As a control, we also
374 analyzed trials with opposite motor intention and congruent somatosensory feedback.
375 We found the activity patterns to differ only slightly with respect to trials with same
376 somatosensory feedback, but opposite motor intention, further showing that
377 somatosensory feedback is prevailing over motor intention after movement onset. In the
378 case of visual feedback (Experiment 1), instead, there was no divergence of activity
379 patterns after the feedback, while trials with different motor intention clearly diverged
380 before the movement onset (see Figure 6A).

381
382 In order to better display the effect of somatosensory feedback on M1 activity for each
383 type of movements, we computed a 2D multidimensional scaling of neural activity as a
384 function of intended movement and congruency of somatosensory feedback. This
385 technique aims at representing the high dimensional spatio-temporal pattern of neural
386 activity in 2D plane, while maximising the fraction of retained variance. As shown in
387 Figure 6C, both for hand (opening/closing) and thumb (flexion/extension) movements,
388 before sensory feedback (in the window between -650 and -150 ms before sensory
389 feedback onset), M1 neural activity is clustered solely as a function of the intended

390 movement. After somatosensory feedback (between 0 and 600 ms from sensory
391 feedback onset, Figure 6D), trials with congruent somatosensory feedback and a given
392 intended movement are clustered more with trials coding for the opposite movement,
393 but receiving the same sensory feedback rather than with trials coding for the same
394 movement.

395 No prior study in humans and only few studies in monkeys directly tested the effects of
396 sensory feedback on BMI performance^{21,25}. Here we show, for the first time, an effect of
397 feedback congruency on BMI performance, and the underlying role of M1 in this
398 process. Our findings indicate that the recorded M1 units processed motor signals for
399 the trained BMI actions, for sensory and sensory-motor signals reflecting the type and
400 congruency of the sensory feedback. Importantly, these processes were found to
401 change across time, as a function of the sensory feedback provided. In particular, our
402 results show that, after somatosensory feedback, the pattern of neural activity from M1
403 reflected more closely the type of movement realized by the NMES (i.e., the pattern of
404 somatosensory feedback) rather than the intended and decoded movement. This re-
405 writing of the encoded M1 movement as a function of the NMES-implemented
406 movement directly relates to the improvement of BMI efficiency based on congruent
407 somatosensory feedback that we observed and was absent in visual feedback trials.

408 This effect might be mediated by mutual connections between the primary motor and
409 the primary somatosensory cortices, which have been extensively documented in non-
410 humans primates²⁶ and in humans²⁷. In addition, this effect might also depend on direct
411 somatosensory inputs reaching M1 neurons likely from the dorsal columns via the
412 ventrolateral thalamic nucleus²⁸. This is an important finding, considering that original
413 BMI approaches for severely motor-impaired patients generally provide visual feedback
414 only^{5,29} or somatosensory feedback by directly stimulating primary somatosensory
415 cortex³⁰⁻³² (see ³¹ *for a review*). Although from a single tetraplegic participant, the
416 present data show that non-invasive somatosensory feedback via NMES not only
417 enables higher subjective feeling of being in control (agency and confidence), but also
418 leads to better actual control of the patient's BMI actions.

419
420 **Agency covaries with BMI classifier.** We finally investigated whether agency has an
421 impact on BMI efficiency and thus tested whether the sense of agency covaried with
422 BMI classifier accuracy. We found that trials with agency versus trials without agency
423 were associated with higher classifier accuracy when somatosensory feedback was
424 modulated (Experiment 2; $t(241) = 8.91$, Cohen's $d = 1.199$, $p < 0.001$), as confirmed
425 from analysis of data from Experiment 3 ($t(446) = 6.256$, Cohen's $d = 0.601$, $p < 0.001$).
426 We found no statistically significant difference between trials with agency and trials
427 without agency in classifier accuracy when visual feedback was modulated (Experiment
428 1; $t(153) = 0.690$, Cohen's $d = 0.111$, $p = 0.49$). In addition, there was a significant
429 correlation across all three experiments between BMI classifier accuracy and
430 confidence (See Supplementary Table 1 for multiple regression analyses). Thus,
431 agency and confidence were both directly related to the performance of the present BMI
432 system, but only when somatosensory feedback was involved. In order to confirm the
433 role of agency on BMI performance, while controlling for other potential factors, we
434 compared the BMI performance between trials in which the BMI user reported high and
435 low agency, within conditions at equivalent sensory feedback, that is V-/S+ and V+/S-
436 from Experiment 3 (which resulted in a balanced and sufficient numbers of trials with
437 "Yes" and "No" responses to Q1). As shown in Figure 5D, BMI accuracy varied as a
438 function of subjective agency judgments, in conditions of equivalent sensory feedback.
439 BMI accuracy was significantly higher in trials with high agency as compared to trials
440 with low agency from 300 ms in the V-/S+ condition. The same pattern is visible in the
441 V-/S+ condition, although the comparison was not significant (i.e., did not survive to
442 correction for multiple comparisons). The same analysis run on confidence ratings (by
443 sorting high and low confidence ratings by means of a median split) did not show any
444 significant difference in BMI accuracy due to confidence at equivalent conditions of
445 sensory feedback (see Supplementary Figure S6). These results suggest that the sense
446 of agency, and not confidence (see Supplementary Table 1 for further analyses), has an
447 effect on BMI accuracy beyond the prominent role of sensory feedback, and impacts
448 BMI accuracy at a later time point. Since agency judgments and confidence ratings
449 reflect two different processes of subjective experience, the present data suggest that

450 pre-reflexive, rather than post-decisional agency components more strongly affect the
451 proficiency of a BMI decoder in M1.

452
453

454 **Discussion**

455 By combining techniques from neurophysiology, neuroengineering, and VR with
456 psychophysics of agency, we were able to study the sense of agency for actions
457 enabled by a BMI-based intracortical neuroprosthesis and found that congruent sensory
458 feedback boosted agency and confidence when controlling BMI actions. Moreover, we
459 showed that human M1 processes not only motor and sensory information, but also
460 different levels of congruency between sensory and motor signals and the resulting
461 sense of agency. The present data are also of clinical relevance, because our NMES-
462 based BMI approach, by providing congruent somatosensory feedback (without direct
463 S1 stimulation) to a tetraplegic patient, improved the ability of the BMI classifier in
464 decoding the patient's motor commands. Interestingly, such higher BMI proficiency was
465 associated with a stronger sense of agency, suggesting that, beyond supporting close-
466 loop systems and M1 feedback in general, somatosensory feedback and signals related
467 to subjective aspects of motor control (i.e., agency) are important input for improving
468 BMI proficiency. Quantifying subjective action-related mental states and including
469 controlled motor and sensory feedback may therefore provide new levels of comfort and
470 personalization and should be considered for the design of future BMIs.

471

472 The present data demonstrate that M1 activity contains information specifically linked to
473 subjective aspects of motor control, in particular the sense of agency and confidence
474 that our participant associated with his BMI actions. It is known that agency likely
475 involves a network of multiple brain areas from which we did not record in the present
476 study (e.g., posterior parietal cortex³³ and angular gyrus; anterior insula^{34,35};
477 supplementary motor cortex³⁶; premotor cortex³⁷; for reviews see ^{3,38}). However, our
478 findings – even if coming from a single tetraplegic patient - directly demonstrate that M1
479 activity contains sufficient information to decode actions for which a human participant
480 feels to be in control. The present BMI findings extend previous research that
481 investigated the sense of agency for non-invasive BCI, as based on scalp

482 electroencephalography (EEG). They add important information about the underlying
483 neural underpinnings based on M1 multiunit activity of the sense of agency in humans.
484 In keeping with a prominent line of research on the role of visuo-motor (and visuo-
485 tactile) cues in boosting or modulating body ownership for artificial and real limbs^{39–42},
486 previous BCI studies also demonstrated that coherent visual feedback results in a
487 higher sense of agency for BCI actions¹⁴. This effect is associated with stronger
488 activations in a cortical-subcortical network, recruited during motor imagery used to
489 control the BCI, consisting of posterior parietal cortex, insula, lateral occipital cortex,
490 and basal ganglia¹³. Another study¹⁰ further demonstrated that a stronger sense of
491 agency for BCI-mediated actions is associated with stronger activity in sensorimotor
492 areas during motor imagery based BCI. The present data on the sense of agency when
493 using an intracortical BMI, although from a single, highly proficient BMI user (see
494 below), demonstrate that this relationship can be tracked down even at the level of
495 multi-unit activity from M1 neurons, and it is further associated with higher BMI
496 proficiency.

497
498 Moreover, the present findings offer a mechanistic explanation for the relationship
499 between sensorimotor activity, sensory feedback and the resulting sense of agency, by
500 showing that M1 activity before movement execution codes for the intended movement,
501 while activity after movement execution encodes the sensory feedback associated with
502 the implemented movement. By showing that somatosensory feedback in particular
503 affects the performance of the BMI classifier, these analyses provide insights into the
504 sensorimotor mechanisms of BMI proficiency. We note that this last finding was
505 possible only due to the combination of a SCI lesion and the present intracortical BMI,
506 which allowed us to decode efferent signals and manipulate afferent signals, not only as
507 visual reproductions of body movements (via VR, as in previous studies), but also as
508 physical movements of the real body (via NMES). In order to highlight the dynamic,
509 multiscale brain mechanisms underlying the sense of agency in humans, future studies
510 should combine insights that can be gained from invasive BMI - with ultra-high spatial
511 resolution, but limited coverage in a handful of subjects – and non-invasive BCI – with
512 limited resolution, but recording from the entire brain in larger subject samples.

513

514 Finally, our results can be of interest not only within the field of neuroprosthetics and its
515 clinical application, but also for basic neuroscience as well as current ethical and legal
516 debates about the subjective sense of agency and responsibility when applying
517 neurotechnology solutions for human repair or enhancement^{38,43,44}.

518
519

520 **Limitations of the study**

521 Because of the uniqueness of the present experimental setup, generalization of the
522 present findings to the general population should be done carefully. First, we tested a
523 single participant, who is an extremely trained BMI user, who could have developed an
524 extraordinary capacity of controlling his BMI system. This could have in turn impacted
525 the associated sense of agency and the discovered links with BMI proficiency. Second,
526 in order to enable movements of his upper limb, we used an NMES system that
527 provides a series of somatosensory cues, which are only partially comparable to those
528 associated with natural movements. For example, the intensity and temporal activation
529 of somatosensory fibers as well as of the recruited motor fibers (antidromic) differs from
530 sensorimotor activation during natural movements. We also note that although our
531 participant suffered severe somatosensory loss (following damage at the C5-C6 level),
532 he may have “learned” to associate some patterns of cutaneous sensations with the
533 specific type of NMES stimulation used to enable specific movements. Indeed, outside
534 of the experimental tasks described here, he was able to identify NMES-implemented
535 movements even without seeing his arm. Finally, given the long-term spinal cord lesion
536 suffered by this participant, we cannot exclude that some plastic changes have occurred
537 in his motor representations in M1, his somatosensory representations in S1, or the
538 connectivity between the two. There is still no consensus about plasticity following
539 spinal cord injury, with some evidence of preserved network organization, some
540 possible changes in grey matter density^{45,46} or activation in the sensorimotor
541 cortices^{47,48}. It is also not clear how these results at the population level of SCI patients
542 are predictive of changes at the single patient level. Thus, at the moment, it is not
543 possible to exclude that some of the present results are idiosyncratic to this particular
544 clinical case.

545

546
547

548 **References**

- 549 1. Blakemore, S. J., Wolpert, D. M. & Frith, C. D. Abnormalities in the awareness of
550 action. *Trends Cogn. Sci.* **6**, 237–242 (2002).
- 551 2. Jeannerod, M. *Motor cognition : what actions tell the self.* (Oxford University
552 Press, 2006).
- 553 3. Haggard, P. Sense of agency in the human brain. *Nat. Rev. Neurosci.* **18**, 196–
554 207 (2017).
- 555 4. Hochberg, L. R. *et al.* Reach and grasp by people with tetraplegia using a neurally
556 controlled robotic arm. *Nature* **485**, 372–375 (2012).
- 557 5. Collinger, J. L. *et al.* High-performance neuroprosthetic control by an individual
558 with tetraplegia. *Lancet* **381**, 557–564 (2013).
- 559 6. Bouton, C. E. *et al.* Restoring cortical control of functional movement in a human
560 with quadriplegia. *Nature* **533**, 247–250 (2016).
- 561 7. Ajiboye, A. B. *et al.* Restoration of reaching and grasping movements through
562 brain-controlled muscle stimulation in a person with tetraplegia: a proof-of-concept
563 demonstration. *Lancet* **389**, 1821–1830 (2017).
- 564 8. Lebedev, M. A. & Nicolelis, M. A. L. Brain-Machine Interfaces: From Basic
565 Science to Neuroprostheses and Neurorehabilitation. *Physiol. Rev.* **97**, 767–837
566 (2017).
- 567 9. Donoghue, J. P. Connecting cortex to machines: recent advances in brain
568 interfaces. *Nat. Neurosci.* **5**, 1085–1088 (2002).
- 569 10. Nierula, B. *et al.* Agency and responsibility over virtual movements controlled
570 through different paradigms of brain–computer interface. *J. Physiol.* **0**, 1–16
571 (2019).
- 572 11. Nierula, B. & Sanchez-Vives, M. V. Can BCI Paradigms Induce Feelings of
573 Agency and Responsibility Over Movements? in (2019). doi:10.1007/978-3-030-
574 05668-1_10.
- 575 12. Sato, A. & Yasuda, A. Illusion of sense of self-agency: Discrepancy between the
576 predicted and actual sensory consequences of actions modulates the sense of
577 self-agency, but not the sense of self-ownership. *Cognition* **94**, 241–255 (2005).
- 578 13. Marchesotti, S. *et al.* Cortical and subcortical mechanisms of brain-machine
579 interfaces. *Hum. Brain Mapp.* **38**, 2971–2989 (2017).
- 580 14. Evans, N., Gale, S., Schurger, A. & Blanke, O. Visual Feedback Dominates the
581 Sense of Agency for Brain-Machine Actions. *PLoS One* **10**, e0130019 (2015).
- 582 15. Knoblich, G. & Sebanz, N. Agency in the face of error. *Trends Cogn. Sci.* **9**, 259–
583 261 (2005).
- 584 16. Tsakiris, M., Prabhu, G. & Haggard, P. Having a body versus moving your body:
585 How agency structures body-ownership. *Conscious. Cogn.* **15**, 423–432 (2006).
- 586 17. Scott, S. H., Cluff, T., Lowrey, C. R. & Takei, T. Feedback control during voluntary
587 motor actions. *Curr. Opin. Neurobiol.* **33**, 85–94 (2015).

- 588 18. Shokur, S. *et al.* Expanding the primate body schema in sensorimotor cortex by
589 virtual touches of an avatar. *Proc. Natl. Acad. Sci.* **110**, 15121–15126 (2013).
- 590 19. Hatsopoulos, N. G. & Suminski, A. J. Sensing with the motor cortex. *Neuron* **72**,
591 477–487 (2011).
- 592 20. Hatsopoulos, N. G., Xu, Q. & Amit, Y. Encoding of movement fragments in the
593 motor cortex. *J. Neurosci.* **27**, 5105–14 (2007).
- 594 21. Suminski, A. J., Tkach, D. C., Fagg, A. H. & Hatsopoulos, N. G. Incorporating
595 Feedback from Multiple Sensory Modalities Enhances Brain-Machine Interface
596 Control. *J. Neurosci.* **30**, 16777–16787 (2010).
- 597 22. Tkach, D., Reimer, J. & Hatsopoulos, N. G. Congruent activity during action and
598 action observation in motor cortex. *J. Neurosci.* **27**, 13241–50 (2007).
- 599 23. Churchland, M. M. & Shenoy, K. V. Temporal Complexity and Heterogeneity of
600 Single-Neuron Activity in Premotor and Motor Cortex. *J. Neurophysiol.* **97**, 4235–
601 4257 (2007).
- 602 24. Schwartz, A. B. Movement: How the Brain Communicates with the World. *Cell*
603 **164**, 1122–1135 (2016).
- 604 25. O’Doherty, J. E. *et al.* Active tactile exploration using a brain–machine–brain
605 interface. *Nature* **479**, 228–231 (2011).
- 606 26. Stepniewska, I., Preuss, T. M. & Kaas, J. H. Architectonics, somatotopic
607 organization, and ipsilateral cortical connections of the primary motor area (M1) of
608 owl monkeys. *J. Comp. Neurol.* **330**, (1993).
- 609 27. Eickhoff, S. B. *et al.* Anatomical and functional connectivity of cytoarchitectonic
610 areas within the human parietal operculum. *J. Neurosci.* **30**, (2010).
- 611 28. Fetz, E. E., Finocchio, D. V., Baker, M. A. & Soso, M. J. Sensory and motor
612 responses of precentral cortex cells during comparable passive and active joint
613 movements. *J. Neurophysiol.* **43**, (1980).
- 614 29. Hochberg, L. R. *et al.* Neuronal ensemble control of prosthetic devices by a
615 human with tetraplegia. *Nature* **442**, 164–171 (2006).
- 616 30. Tabot, G. A. *et al.* Restoring the sense of touch with a prosthetic hand through a
617 brain interface. *Proc. Natl. Acad. Sci. U. S. A.* **110**, 18279–84 (2013).
- 618 31. Flesher, S. N. *et al.* Intracortical microstimulation of human somatosensory cortex.
619 *Sci. Transl. Med.* **8**, 361ra141 LP-361ra141 (2016).
- 620 32. Bensmaia, S. J. & Miller, L. E. Restoring sensorimotor function through
621 intracortical interfaces: progress and looming challenges. *Nat. Rev. Neurosci.* **15**,
622 313–325 (2014).
- 623 33. Desmurget, M. *et al.* Movement intention after parietal cortex stimulation in
624 humans. *Science* **324**, 811–3 (2009).
- 625 34. Farrer, C. & Frith, C. D. Experiencing Oneself vs Another Person as Being the
626 Cause of an Action: The Neural Correlates of the Experience of Agency.
627 *Neuroimage* **15**, 596–603 (2002).

- 628 35. Chambon, V., Wenke, D., Fleming, S. M., Prinz, W. & Haggard, P. An online
629 neural substrate for sense of agency. *Cereb. Cortex* **23**, 1031–1037 (2013).
- 630 36. Fried, I., Mukamel, R. & Kreiman, G. Internally Generated Preactivation of Single
631 Neurons in Human Medial Frontal Cortex Predicts Volition. *Neuron* **69**, 548–562
632 (2011).
- 633 37. Fornia, L. *et al.* Direct electrical stimulation of the premotor cortex shuts down
634 awareness of voluntary actions. *Nat. Commun.* **11**, 1–11 (2020).
- 635 38. Sperduti, M., Delaveau, P., Fossati, P. & Nadel, J. Different brain structures
636 related to self- and external-agency attribution: A brief review and meta-analysis.
637 *Brain Struct. Funct.* **216**, 151–157 (2011).
- 638 39. Blanke, O., Slater, M. & Serino, A. Behavioral, Neural, and Computational
639 Principles of Bodily Self-Consciousness. *Neuron* **88**, 145–166 (2015).
- 640 40. Makin, T. R., Holmes, N. P. & Ehrsson, H. H. On the other hand: Dummy hands
641 and peripersonal space. *Behav. Brain Res.* **191**, 1–10 (2008).
- 642 41. Rognini, G. *et al.* Multisensory bionic limb to achieve prosthesis embodiment and
643 reduce distorted phantom limb perceptions. *J. Neurol. Neurosurg. Psychiatry* **90**,
644 833–836 (2019).
- 645 42. Sanchez-Vives, M. V., Spanlang, B., Frisoli, A., Bergamasco, M. & Slater, M.
646 Virtual hand illusion induced by visuomotor correlations. *PLoS One* **5**, e10381
647 (2010).
- 648 43. Yuste, R. *et al.* Four ethical priorities for neurotechnologies and AI. *Nature* **551**,
649 159–163 (2017).
- 650 44. Fried, I., Haggard, P., He, B. J. & Schurger, A. Volition and Action in the Human
651 Brain: Processes, Pathologies, and Reasons. *J. Neurosci.* **37**, 10842–10847
652 (2017).
- 653 45. Wang, W. *et al.* Specific Brain Morphometric Changes in Spinal Cord Injury: A
654 Voxel-Based Meta-Analysis of White and Gray Matter Volume. *J. Neurotrauma*
655 **36**, (2019).
- 656 46. Melo, M. C., Macedo, D. R. & Soares, A. B. Divergent Findings in Brain
657 Reorganization After Spinal Cord Injury: A Review. *Journal of Neuroimaging* vol.
658 30 (2020).
- 659 47. Freund, P. *et al.* MRI investigation of the sensorimotor cortex and the
660 corticospinal tract after acute spinal cord injury: A prospective longitudinal study.
661 *Lancet Neurol.* **12**, (2013).
- 662 48. Henderson, L. A., Gustin, S. M., Macey, P. M., Wrigley, P. J. & Siddall, P. J.
663 Functional reorganization of the brain in humans following spinal cord injury:
664 Evidence for underlying changes in cortical anatomy. *J. Neurosci.* **31**, (2011).
- 665 49. Mallat, S. *A Wavelet Tour of Signal Processing. A Wavelet Tour of Signal*
666 *Processing* (2009). doi:10.1016/B978-0-12-374370-1.X0001-8.
- 667 50. Humber, C., Ito, K. & Bouton, C. Nonsmooth Formulation of the Support Vector
668 Machine for a Neural Decoding Problem. *arXiv* (2010).

- 669 51. Colachis, S. C. *et al.* Dexterous control of seven functional hand movements
670 using cortically-controlled transcutaneous muscle stimulation in a person with
671 tetraplegia. *Front. Neurosci.* **12**, 1–14 (2018).
- 672 52. Colachis, S. C. I. Optimizing the Brain-Computer Interface for Spinal Cord Injury
673 Rehabilitation. (2018).
- 674 53. Zhang, M. *et al.* Extracting wavelet based neural features from human intracortical
675 recordings for neuroprosthetics applications. *Bioelectron. Med.* **4**, 11 (2018).
- 676 54. Quiroga, R. Q., Nadasdy, Z. & Ben-Shaul, Y. Unsupervised Spike Detection and
677 Sorting with Wavelets and Superparamagnetic Clustering. *Neural Comput.* **16**,
678 1661–1687 (2004).
- 679 55. Hoerl, A. E. & Kennard, R. W. Ridge Regression: Biased Estimation for
680 Nonorthogonal Problems. *Technometrics* **12**, 55–67 (1970).
- 681 56. Kuhn, M. R Package: caret, Ver. 6.0-80. *CRAN* (2018).
- 682 57. Maris, E. & Oostenveld, R. Nonparametric statistical testing of EEG- and MEG-
683 data. *J. Neurosci. Methods* **164**, 177–190 (2007).
- 684
- 685

686 **Acknowledgments**

687 The authors thank Ian for his dedication to the study and insightful conversations.

688 AS is supported by the Swiss National Science Foundation (grant (PP00P3_163951 /
689 1), OB is supported by the Swiss National Science Foundation and the Bertarelli
690 Foundation. MB is supported by the Craig H. Neilsen Foundation (Grant
691 number: 651289) and State of Ohio Research Incentive Third Frontier Fund. The
692 funders had no role in study design, data collection and analysis, decision to publish or
693 preparation of the manuscript.

694

695 **Author contributions** AS: Conceptualization, Formal Analysis, Methodology, Writing;
696 *MB*: Methodology, Investigation, Project Administration, Review & Editing; TB: Data
697 curation, Formal analysis, Software, Visualization, Review & editing; SC: Methodology,
698 Data Curation, Formal analysis, Investigation, Software; MS: Formal analysis,
699 Investigation, Visualization, Review & editing; CD, KE: Investigation, Data collection PG:
700 Methodology, Review & Editing; GS: Methodology, Software and Hardware
701 development; NA: Methodology, Review & editing; PO: Investigation, Software and
702 Hardware development, DF: Investigation, Software and Hardware development, PS:
703 Methodology, Review & editing; NF: Formal analysis, Methodology, Visualization,
704 Review & editing; AR: Funding acquisition, Resources, Supervision, Review & editing;
705 OB: Conceptualization, Funding acquisition, Methodology, Supervision, Writing.

706

707 **Competing interests:** AS, MS, TB, NF, PS, and OB declare no competing interests.
708 CD, KE, PG, GS, NA, and DF hold patents for the BMI system.

709

710 **Figure legends**

711

712 **Figure 1. Experimental setup.** A. Events during trials. One (out of four possible
713 movements) was cued, following a “Go” signal to initiate the movement. The BMI
714 classifier decoded the movement from M1 activity and sensory feedback was given. The
715 patient answered two questions: Q1. “Are you the one who generated the movement?”,
716 by saying “Yes” or “No”; and Q2. “How confident are you?”, by indicating a number
717 ranging from 0 (absolutely unsure) to 100 (absolutely sure). B: Example of sensory
718 feedback for one type of movement. The chosen movement was realized as a visual
719 feedback, via virtual reality (VR – Experiment 1), as a somatosensory feedback, via
720 NEMS (Experiment 2) or both (Experiment 3). In different congruency conditions, either
721 the cued and correctly decoded movement (Congruent) or the opposite movement
722 (Incongruent) was realized for the different modalities. The location of the electrodes
723 array in the M1, with respect to the pattern of activity for upper limb attempted
724 movement from fMRI is also shown (from ⁶).

725

726 **Figure 2. Agency judgements and confidence depends on sensory feedback.** A.
727 Proportion of “Yes” and “No” answers (Q1) to congruent and incongruent trials for the
728 visual (Experiment 1) somatosensory (Experiment 2) and the combination of the two
729 modalities (Experiment 3). B-C-D: Confidence about agency judgments. Distribution of
730 Q2 responses as a function of the congruency of visual (B), somatosensory (C) or both
731 (D) sensory feedback.

732

733 **Figure 3. M1 activity depends on sensory feedback.** Sensory feedback as encoded
734 by Local field potentials (LFP; left panel) and Multiunit firing rates (MU; right panel). LFP
735 and MU modulation for congruent and incongruent visual (Experiment 1) and
736 somatosensory (Experiment 2) feedback (A) and for the combination of the two
737 (Experiment 3, B). Colored lines represent averaged signal across all channels (shaded
738 areas indicate SEMs); black lines report the time-related k-values of the multivariate
739 decoder distinguishing between congruent and incongruent feedback; the underlying
740 thick segments indicate k-values significantly higher than chance level from cluster-
741 based permutation analyses.

742

743 **Figure 4. Sense of agency in M1.** Sense of agency as coded by LFP (left) and Multi-
744 unit firing rates (right). A. Left and right panels respectively show averaged LFP and
745 Multi-unit modulation for high (green) and no (grey) agency response to Q1 (shaded
746 areas indicate SEMs); black lines report the time-related k-values of the multivariate
747 decoder distinguishing the two conditions; the underlying thick segments indicate k-
748 values significantly higher than chance level from cluster-based permutation analyses.
749 B: Results of the decoder discriminating between high vs. low orthogonalized agency
750 scores from LFP (left) and MU (right) after regressing out for the effects of the
751 congruency of sensory feedback and type of movements.

752

753 **Figure 5. Performance of BMI classifier as a function of sensory feedback and**
754 **sense of agency.** A-B-C. The left panels (A, B, C) show the modulation in time of the
755 performance of the BMI classifier for the 4 types of movements indicated for the cued
756 movement (filled line) and the opposite (dashed line), as a function of feedback (i.e.
757 black dots indicate time points with significant difference). The right panels show the
758 area under the curve taken as an index of global performance of the BMI. The
759 performance of the BMI classifier does vary not as a function of visual feedback
760 (Experiment 1, A), but it is significantly better when somatosensory feedback is
761 congruent both in Experiment 2 (B) and in Experiment 3 (C). D. BMI accuracy in time as
762 a function of sense of agency. Blue/red curves represent the BMI classifier output for
763 the cued movement as a function of agency judgements (Q1: 1=high agency; 0=low
764 agency) in conditions of equal sensory feedback.

765

766

767 **Figure 6. Somatosensory feedback changes firing rates of M1 neurons. A-B.**
768 Euclidean distance in time between trials with same motor intention and opposite
769 feedback (red), same feedback and opposite intention (blue), or opposite congruent
770 feedback and intention (green), for experiment 1 (A) and 2 (B). In Experiment 1, neural
771 activity diverged as a function of motor intention before the movement, as shown by the
772 increase in Euclidean distances between the green and blue curves. In Experiment 2,
773 neural activity diverged as function of sensory feedback after NMES activation. **C-D.**

774 Multidimensional scaling of neural activity before (-650/150 ms; C) and after (0/500 ms;
775 D) sensory feedback. The plots show a 2D dimensionality reduction of population
776 activity in the target period, in order to represent it on a plane. As in a principal
777 component analysis, Dimensions 1 and 2 can be seen as the two abstract coordinates
778 explaining most variance in the data. Movements are separated by classes of hand
779 (open/close; right) and thumb (extension / flexion; left) movements.

780

781

782

783

784

785 **Materials and Methods**

786 **Participant**

787 The participant in this study was enrolled in a pilot clinical trial (NCT01997125) of a
788 custom neural bridging system (Battelle Memorial Institute) to reanimate paralyzed
789 upper limbs after C4-6 spinal cord injury. The system consisted of a Neuroport data
790 acquisition system (Blackrock Micro, Salt Lake, Utah), custom signal processing and
791 decoding algorithms (Battelle), and a NeuroLife Neuromuscular Stimulation System
792 (Battelle). The trial received investigational device exemption (IDE) approval by the US
793 Food and Drug Administration and Institutional Review Board approval through the Ohio
794 State University (Columbus, Ohio). The study conformed to institutional research
795 requirements for the conduct of human subjects. The site of the experiments was the
796 Ohio State University NeuroRehabLab (Bockbrader, PI) and data was analyzed at Ohio
797 State (Columbus, Ohio) and École polytechnique fédérale de Lausanne (EPFL,
798 Switzerland). The participant provided informed consent at the time of enrollment and
799 also provided written permission for photographs and videos.

800 The study participant was a 22 year-old male at the time of study enrollment. He had
801 complete C5 ASIA A, non-spastic tetraparesis from cervical spinal cord injury
802 associated with a diving accident 3 years prior. On neurological exam, he had full motor
803 function bilaterally for C5 level muscles (e.g., biceps and shoulder girdle muscles), but
804 no motor function below the C6 level. He had 1/5 strength on the right and 2/5 strength
805 on the left for wrist extension (C6 level) on manual muscle testing. His sensory level
806 was C6 on the left and C5 on the right, although he had sensation for pressure on his
807 right thumb. He had preserved proprioception for shoulder, elbow and wrist joint
808 position, but was at chance level for distinguishing digit joint positions
809 (flexion/neutral/extension) for the thumb and fingers. He had mild finger flexor
810 contractures bilaterally, limiting finger extension at the proximal and distal
811 interphalangeal joints of digits 2-5.

812 He was implanted with a 4.4 x 4.2mm intracortical silicon Neuroport microelectrode
813 array (Blackrock Microsystems) in the dominant hand/arm area of his motor cortex on
814 4/22/2014, as previously described⁶. The implant site was determined by preoperative
815 functional neuroimaging obtained while the participant visualized movements of his right

816 hand and forearm. He began using cortically-controlled transcutaneous neuromuscular
817 electrical stimulation (NMES) on his right forearm on 5/23/14. Data for this study was
818 collected over 13 sessions (45 hours) from 11/16/2016 - 2/20/2017, corresponding to
819 post-implant days 939-1035. One session with visual and NMES feedback was used for
820 practice (5 blocks of 32 trials on post-implant day 939). At the time of data collection,
821 the participant was an expert brain-machine interface (BMI) user with over 800 hours of
822 study participation.

823 The participant underwent cognitive testing approximately one year after Utah array
824 implantation (January – July, 2015). He scored with superior verbal abilities, attention,
825 and working memory (ranging between 92nd - 99th percentile for his age).

826

827 **Cortical Signal Acquisition and Classification**

828 Neural data (96 channels) were acquired from the left motor cortex Utah array through
829 the Neuroport data acquisition system (Blackrock Micro). Raw data were processed
830 using analog hardware with 0.3Hz 1st order high-pass and 7.5kHz 3rd order Butterworth
831 low-pass filters, then digitized at 30,000 Hz. Data were divided into 100ms bins and
832 passed into Matlab (version 2014b), where signal artifact was removed by blanking over
833 3.5ms around artifacts (defined as signal amplitude >500 μ V at the same time on 4 of 12
834 randomly-selected channels). Signals were decomposed into mean wavelet power
835 (MWP) using the 'db4' wavelet over 100ms⁴⁹. Coefficients within the multiunit frequency
836 bands (234–3,750Hz, coefficients of scales 3, 4, 5, 6) were averaged across the 100ms
837 window and normalized by channel (by subtracting the mean and dividing by the
838 standard deviation of each channel and scale, respectively). Normalized coefficients for
839 each channel were averaged across scales 3-6, creating 96 MWP values (one for each
840 channel) per each 100ms. MWP values were fed as features into a real-time, nonlinear
841 support vector machine (SVM) classifier⁵⁰ with five classes (hand open, hand closed,
842 thumb extension, thumb flexion, and rest). Classifier activation values were computed
843 for each 100ms bin and ranged from -1 to 1. Classifier output represented the
844 movement pattern (hand open, hand closed, thumb extension, thumb flexion) with the
845 highest activation greater than threshold (zero). If no movement classes had activation

846 greater than zero, the classifier was in the “rest” state. If multiple output classes
847 exceeded threshold, only the one with the highest score was used to provide feedback.
848 Signal quality was stable⁵¹ during the interval of data collection; but represented about a
849 30% decline in MWP normalized to post-implant 87⁵². (See below for single unit
850 statistics.) Average impedance was approximately 200 k Ω , a decline of 40% of its initial
851 value. Average signal-to-noise was approximately 17.5dB, a decrease of about 10% of
852 its initial value⁵³. Most of the decline in signal quality occurred in the first 400 days post-
853 implantation.

854

855 **Classifier Training and Neurally Controlled Hand Movements**

856 Before each session, the SVM classifier was trained in an adaptive manner over 5
857 blocks. Each block consisted of 3 repetitions of 4 movements (hand open, hand closed,
858 thumb extension, thumb flexion) presented in a random order. Movements were cued
859 for 3-4s (4-5s inter-cue interval) using a small, animated hand in the corner of the video
860 display. Feedback was given with both NMES and the feedback hand on the video
861 screen. During the first training block, scripted feedback was provided simultaneously
862 with the cued movements. In subsequent blocks, appropriate movements were
863 activated when an output class for a given movement exceeded threshold (>0).
864 Training took approximately 10-15 minutes per session.

865

866 **Neuromuscular Electrical Stimulation**

867 The NMES system was used to evoke hand and finger movements by stimulating
868 forearm muscles. The system consisted of a multi-channel stimulator and a flexible,
869 130-electrode, circumferential forearm cuff. Coated copper electrodes with hydrogel
870 interfaces (Axelgaard, Fallbrook, CA) were 12mm in diameter, spaced at regular
871 intervals in an array (22mm longitudinally X 15mm transversely), and delivered current
872 in monophasic, rectangular pulses at 50Hz (pulse width 500 μ s, amplitude 0-20mA).
873 Desired hand/finger movements were calibrated at the beginning of each session by
874 determining/confirming the intensity and pattern of electrodes required to stimulate
875 intended movements. This took 5-10 minutes per session.

876 During the experiment, the participant's view of NMES-evoked movements was
877 obscured from view by the video display. During Experiment 1, non-informative NMES
878 feedback was given (current at an intensity equivalent to what was used for movement
879 calibration patterns, but that did not evoke movement). During Experiments 2 and 3,
880 NMES feedback was provided that evoked hand and finger movements.

881

882 **Virtual Reality Animation**

883 A non-immersive virtual reality system (i.e. without a head-mounted display or head-
884 tracking) was used to provide visual feedback. This was done in order to adopt a
885 previous setup that the participant was already familiar with to the present experiments
886 and also facilitated the calibration procedure to train the BMI classifier. A physics-based
887 animated hand was used to provide visual feedback of classifier activation. During
888 training, two animated hands were displayed, a small cue hand at the bottom left and a
889 larger centrally-placed feedback hand (Figure 1 main text). During the experiment, the
890 display was oriented over the participant's forearm, a single, centrally-placed feedback
891 hand was displayed to match the size and location of the participant's right hand (the
892 cue hand was not displayed). During Experiments 1 and 3, feedback was provided
893 using the virtual hand. During Experiment 2, non-informative visual feedback was given
894 (the feedback hand remained in a neutral, rest position).

895

896 **Feedback Congruency**

897 In half of the trials across Experiments, the visual and/or somatosensory feedback was
898 covertly manipulated to be incongruent with the cue. In incongruent trials, when the
899 participant correctly activated the classifier associated with the cue, he received
900 feedback opposite to the cue (i.e., hand closed for "hand open", thumb extension for
901 "thumb flex", etc.). In congruent trials, he received feedback consistent with the cue
902 (i.e., hand open for "hand open", thumb flexion for "thumb flex", etc.).

903

904 **Agency Assessment**

905 All experimental trials began with a verbal cue ("hand open", "hand closed", "thumb
906 extend", "thumb flex"), followed by a 2 second delay, then a verbal cue ("go"). During
907 the next 4s, the participant was given feedback based on classifier activation levels, and

908 then was told to “stop”). Over the next 5-5.5s, the participant reported whether he felt in
909 control of the movement (“yes” or “no”) and his degree of certainty (0-100). The next
910 trial began at the end of this 5-5.5s interval. There were 32 trials per block in
911 Experiments 1 and 2 and 26 trials per block in Experiment 3.

912

913 **Trial Selection and Time-locking**

914 To ensure that the participant was successfully activating the classifier for the cued
915 movement, and the signal can be meaningfully time-locked to movement onset, we
916 applied the following selection criteria on the trials. We consider it as a correct imagined
917 movement when the participant is able to maintain the classifier of the cued movement
918 above the threshold for at least 600 ms (6 classifier output bins). We retain trials in
919 which at least one correct movement happens between the GO cue and 1.5 seconds
920 before the STOP cue. Epochs are then constructed by time-locking every trial with
921 respect to the onset of such imagined movements. In case several correct movements
922 occurred during the same trial, the time-locking is relative to the first movement.
923 Furthermore, we excluded 128 trials from the session on which the participant
924 systematically reported problems with controlling the BMI system and absent subjective
925 agency. Globally, we retained 846 out of 1408 trials (60%).

926 Note that, since we define the onset as the beginning of the 100 ms bin of neural activity
927 that is fed to the classifier, and around 50 ms are required to compute the output, the
928 corresponding feedback is received about 150 ms after the onset of the imagined
929 movement.

930

931 **Experiment 1: Agency Assessment with Virtual Hand Feedback and Non-** 932 **informative NMES**

933 Twelve blocks of 32 trials were collected on post-implant days 953 (4 blocks), 988 (4
934 blocks), and 1035 (4 blocks). In each trial, the participant received a verbal cue to
935 perform a movement (“hand open”, “hand closed”, “thumb extend”, “thumb flex”). When
936 a classifier crossed threshold during the 4 second feedback window, feedback was
937 given by showing movement of the virtual hand and by activating non-informative NMES
938 (radial wrist electrode activation that did not elicit movement, did not vary from trial to
939 trial, and that the participant could feel and distinguish from real NMES feedback).

940 Feedback on half of the trials was randomly selected to be incongruent with the cue. His
941 subjective sense of agency and level of certainty were recorded for each trial.

942 A total of 384 trials were collected across three days. After removing trials where the
943 cued action could not be correctly decoded and the session on post-implant day 1035
944 (see trial selection paragraph), 83 congruent and 72 incongruent trials remained for
945 behavioral and neural activity analysis.

946

947 **Experiment 2: Agency Assessment with NMES Feedback and Non-informative** 948 **Virtual Hand**

949 Twelve blocks of 32 trials were collected on post-implant days 941 (5 blocks), 960 (3
950 blocks), and 967 (4 blocks). In each trial, the participant received a verbal cue to
951 perform a movement (“hand open”, “hand closed”, “thumb extend”, “thumb flex”). When
952 a classifier crossed threshold during the 4 second feedback window, feedback was
953 given by activating movement of the participant’s hand and wrist through NMES and
954 showing non-informative visual feedback (non-moving hand). The participant could not
955 see his own hand/wrist, but could distinguish his hand state based what the stimulation
956 patterns felt like to him. Feedback on half of the trials was randomly selected to be
957 incongruent with the cue. His subjective sense of agency and level of certainty were
958 recorded for each trial.

959 A total of 384 trials were collected across three days. After removing trials where the
960 participant did not respond correctly by activating the classifier associated with the cue,
961 154 congruent and 89 incongruent trials remained for behavioral and neural activity
962 analysis.

963

964 **Experiment 3: Agency Assessment with Virtual Hand and NMES Feedback**

965 Twenty blocks of 32 trials were collected on post-implant days 993 (3 blocks), 990 (5
966 blocks), 1007 (4 blocks), 1014 (3 blocks), and 1021 (5 blocks). In each trial, the
967 participant received a verbal cue to perform a movement (“hand open”, “hand closed”,
968 “thumb extend”, “thumb flex”). When a classifier crossed threshold during the 4 second
969 feedback window, feedback was given by activating movement of the participant’s hand
970 and wrist through NMES and showing movement of the virtual hand. The participant
971 could not see his own hand/wrist, but could distinguish his hand state based what the

972 stimulation patterns felt like to him. Congruency with respect to the cue was
973 manipulated independently in the visual and somatosensory modalities such that 25%
974 of the trials were each: congruent for both visual and NMES feedback, incongruent for
975 both visual and NMES feedback, congruent for visual but incongruent for NMES
976 feedback, congruent for NMES but incongruent for visual feedback. His subjective
977 sense of agency and level of certainty were recorded for each trial.

978 A total of 520 trials were collected across five days. After removing trials where the
979 participant did not respond correctly by activating the classifier associated with the cue,
980 the number of trials that remained for behavioral and neural activity analysis were: 117
981 congruent for both visual and NMES feedback, 103 incongruent for both visual and
982 NMES feedback, 101 congruent for visual and incongruent for NMES feedback, and
983 127 congruent for NMES and incongruent for visual feedback.

984

985 **Firing Rate Calculation and Single Unit Analyses**

986 Single units were identified through offline data processing. For each block, raw voltage
987 recordings at each channel were processed in a series of steps. First, FES stimulation
988 artifact was removed using a 500 μ V threshold and 3.5ms artifact removal time window.
989 The removed window was replaced with an interpolated segment to retain temporal
990 information. Then, the raw signal with FES artifact removed was processed with a 300-
991 3000Hz bandpass filter. The filtered data was fed into an automated spike detection and
992 sorting algorithm, wave_clus⁵⁴ using the default optimization settings. A threshold was
993 set to four times the standard deviation of the noise and used to detect spike locations.
994 A wavelet decomposition was performed on the spikes to extract features and a
995 superparamagnetic clustering algorithm was used to cluster the spikes into groups,
996 representative of individual single units. The superparamagnetic clustering algorithm
997 was used to eliminate spikes that were considered noise to ensure only single units
998 were analyzed. As spike sorting was not performed before data collection, there was no
999 way to match single units across days. Additionally, the number of single units detected
1000 at a given channel fluctuated between days, possibly due to micro-movement of the
1001 array and brain state changes. For this reason, all single units detected at a given
1002 channel were considered the same and pooled at the single channel level as multiunit
1003 activity in subsequent analysis.

1004

1005 **Offline neural decoding**

1006 Sensory feedback congruency and subjective ratings (Q1 and Q2) were decoded offline
1007 both from LFPs and from multiunit activity. For LFP analysis, the signal amplitude for
1008 each channel was downsampled to 500 Hz, band-passed between 0.1 and 12 Hz with
1009 an IIR filter and smoothed using sliding averaging windows of 250 ms. Following
1010 multiunit spike times calculation (see above), multiunit firing rate was estimated at 20 Hz
1011 over a 250 ms sliding window.

1012 We fed each channel's signal amplitude (LFP) or firing rate (multiunit) as predictors to a
1013 penalized linear decoder based on ridge regressions⁵⁵. A separate model was trained to
1014 decode congruency (Q1) or confidence (Q2) on each signal timepoint, with a sampling
1015 rate of 20 and 500 Hz for multiunit and LFPs respectively. Decoding performance was
1016 evaluated by computing and averaging Cohen's k (logistic regression; Q1) or R^2 (linear
1017 regression; Q2) values over 10 independent 10-fold cross validation runs. The
1018 regression was performed through the "train" function of the R "caret" package⁵⁶. To
1019 evaluate the statistical significance of the decoding, we generated a null decoding
1020 performance distribution by applying the same decoding methods on the data after
1021 randomly shuffling Q1 and Q2 values. 1000 permutations were generated, and the
1022 decoding performance was evaluated for each of them. Then, a t-value was assigned to
1023 every time-point both in real and permuted data, by comparing its decoding
1024 performance to the null distribution of permuted data. Finally, the t-values were used to
1025 define significant decoding time windows based on a cluster-based permutation test on
1026 each epoch's largest cluster⁵⁷. After checking that the t-value threshold used to define
1027 clusters was not significantly affecting the results, its value was set at 2.

1028

1029 **Computation of distance between neural activity patterns**

1030 Since the neural activity recorded by the microelectrode array can change significantly
1031 between experimental sessions (i.e., days of recording) spanned by our analysis,
1032 Euclidean distances per each pair of conditions were computed separately within each
1033 day of recording and then averaged to obtain the final results. Confidence intervals were
1034 obtained through a bootstrapping technique, again applied within sessions. For each

1035 session and condition, we extracted n random trials with replacement, where n is the
1036 number of trials for that condition/session, and the final Euclidean distance was
1037 obtained by averaging across sessions as described above. The procedure was
1038 repeated 100 times, and 95 % confidence intervals were obtained as 1.96 times the
1039 standard deviation of the surrogated distribution obtained as explained here.

1040

1041 **Multidimensional scaling**

1042 In order to graphically represent the spatio-temporal patterns of neural activity, we
1043 performed a multidimensional scaling (MATLAB function mds) on correlation distances
1044 computed between spatio-temporal patterns of neural activity. Also, in this case, to
1045 avoid including sources of variances due to the change in signal between experimental
1046 sessions, the procedure was run within experimental sessions. In order to obtain
1047 correlation distances between trials we started by concatenating, for each trial, data
1048 from all channels and timepoints within the selected temporal window. Then, we
1049 computed the correlation coefficient of the resulting vector with the equivalent vector
1050 from all other trials within the same session and subtracted the obtained values to 1 to
1051 obtain values of the correlation distance. The first two dimensions of the
1052 multidimensional scaling were then aligned across sessions via the Procrustes analysis
1053 (MATLAB function Procrustes), using the means by conditions (combinations of
1054 movement/somatosensory feedback) in the first session as a reference.

1055

1056

1057 **Data availability statement**

1058

1059 Behavioral data and processed data necessary to reproduce the figures in the main text
1060 can be found in the OSF repository accessible at:

1061 https://osf.io/7rma5/?view_only=9928bd8e32a748828f7ecfdbeb1f8baa.

1062 Neural data and code for BMI control can be made available to qualified individuals for
1063 collaboration via a written agreement between Battelle Memorial Institute and the
1064 requester's affiliated institution. Such inquiries or requests should be directed to:

1065 ganzer@battelle.org.

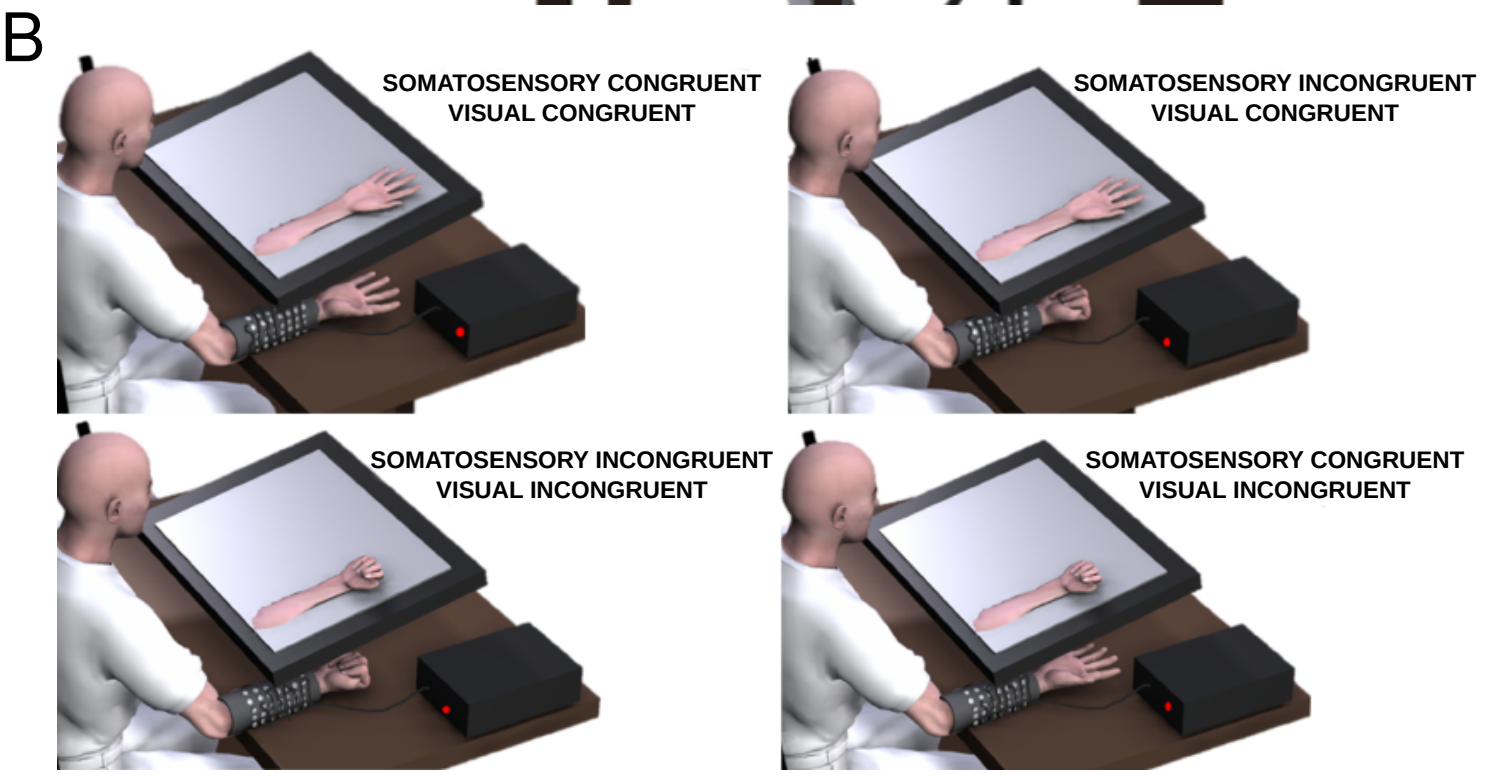
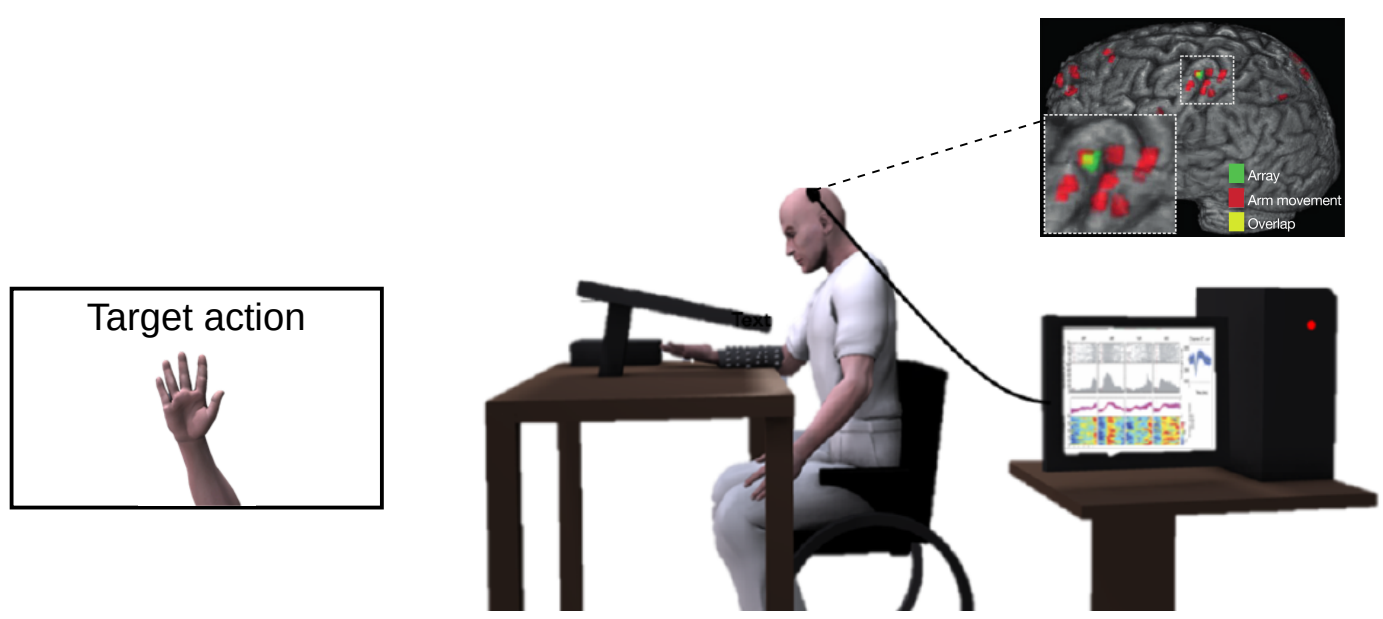
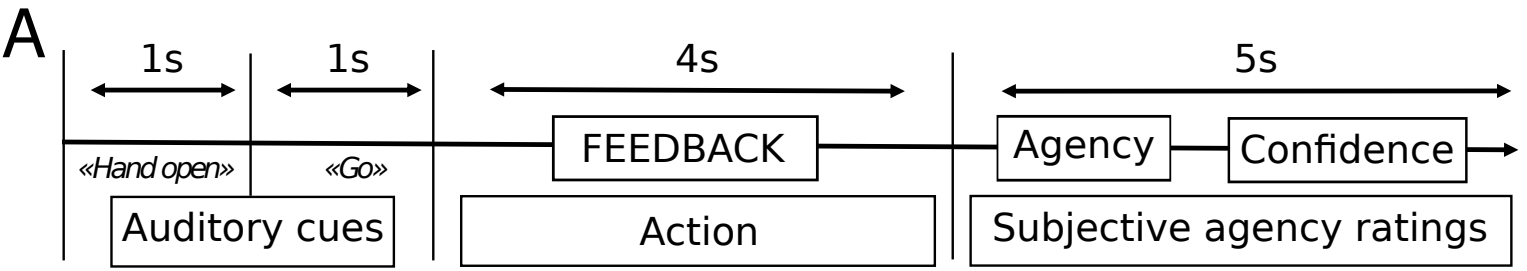
1066

1067 **Code availability statement**

1068

1069 Custom code for neural data analysis and BMI control can be obtained following a
1070 written agreement between Battelle Memorial Institute and the requester's affiliated
1071 institution. Such inquiries or requests should be directed to: ganzer@battelle.org.
1072 Inquiries or requests concerning custom analysis code used for this study should be
1073 directed to AS.

1074

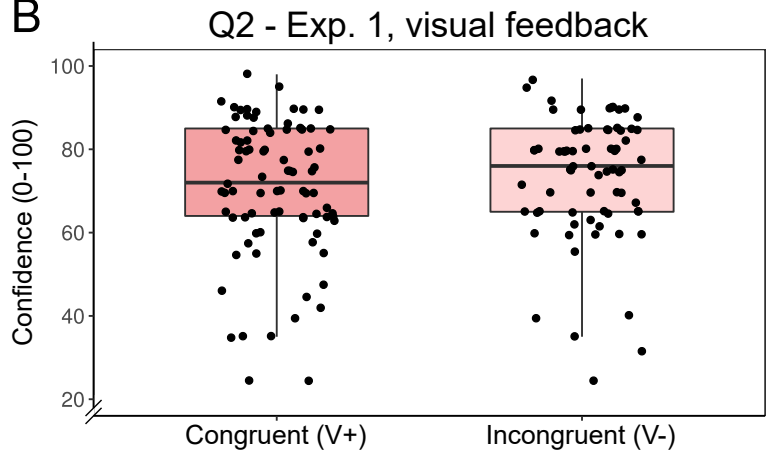
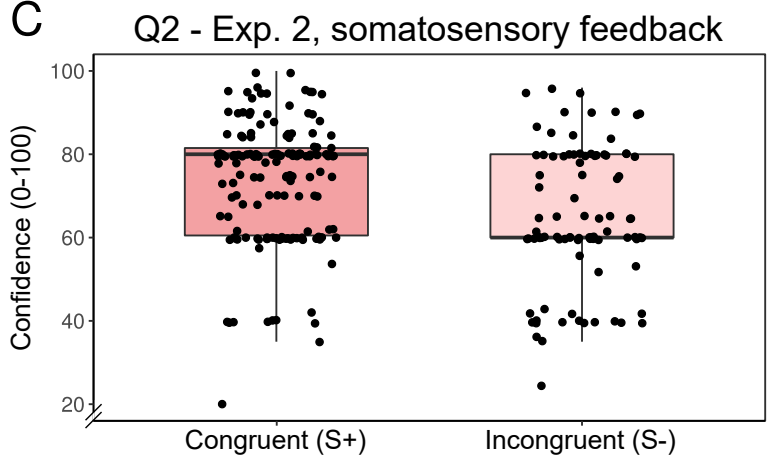
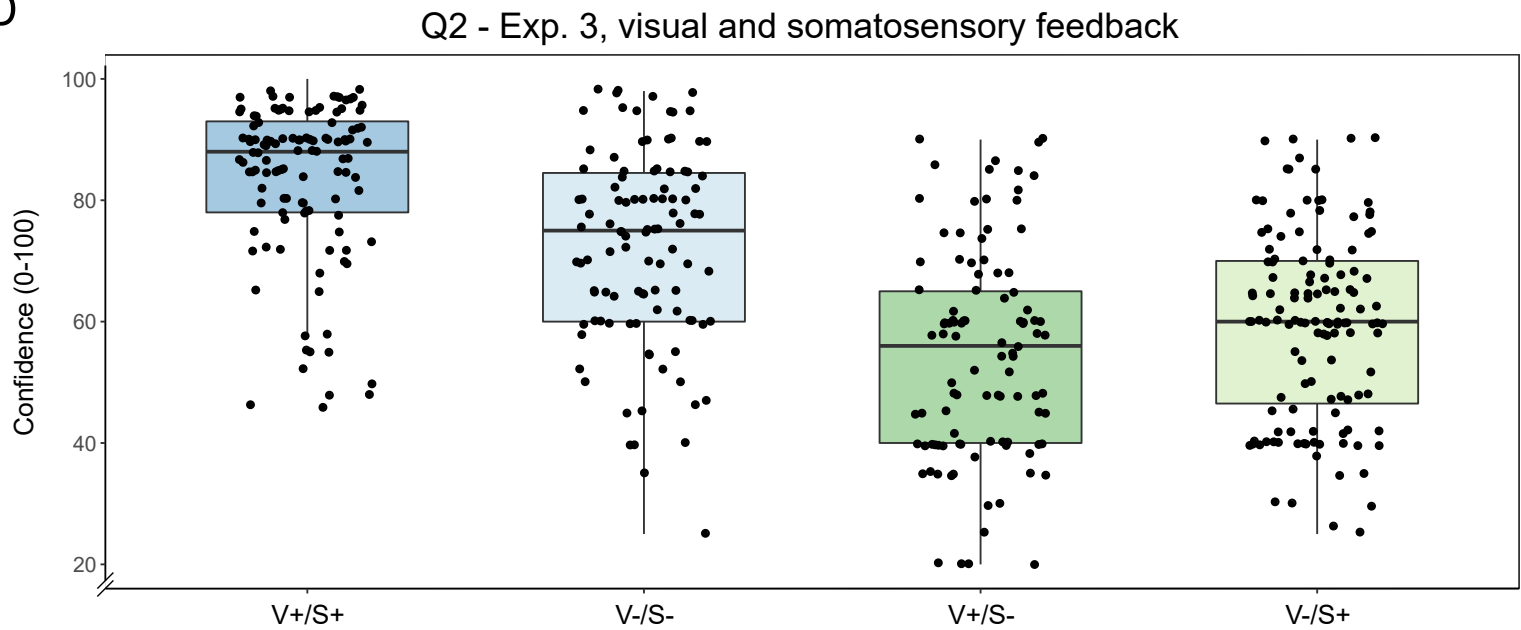


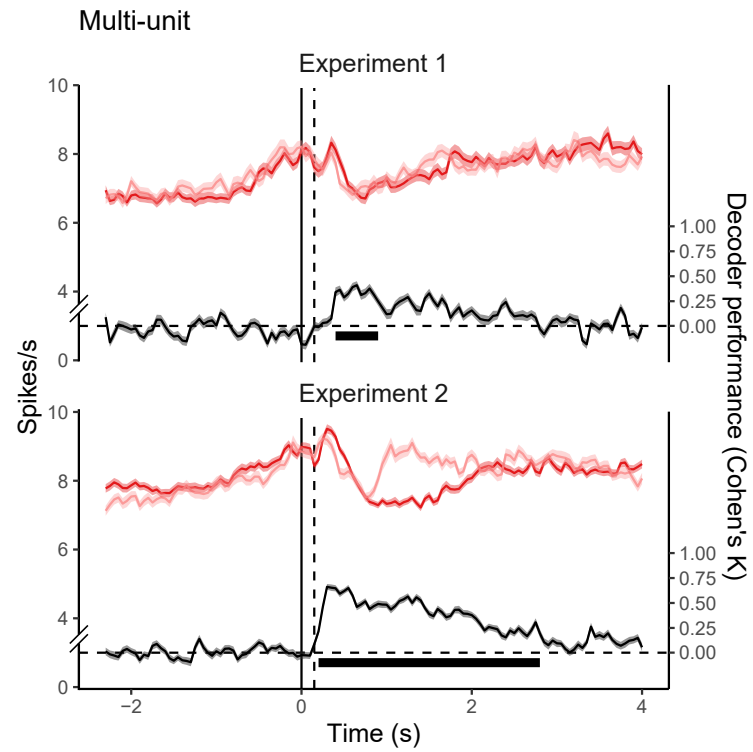
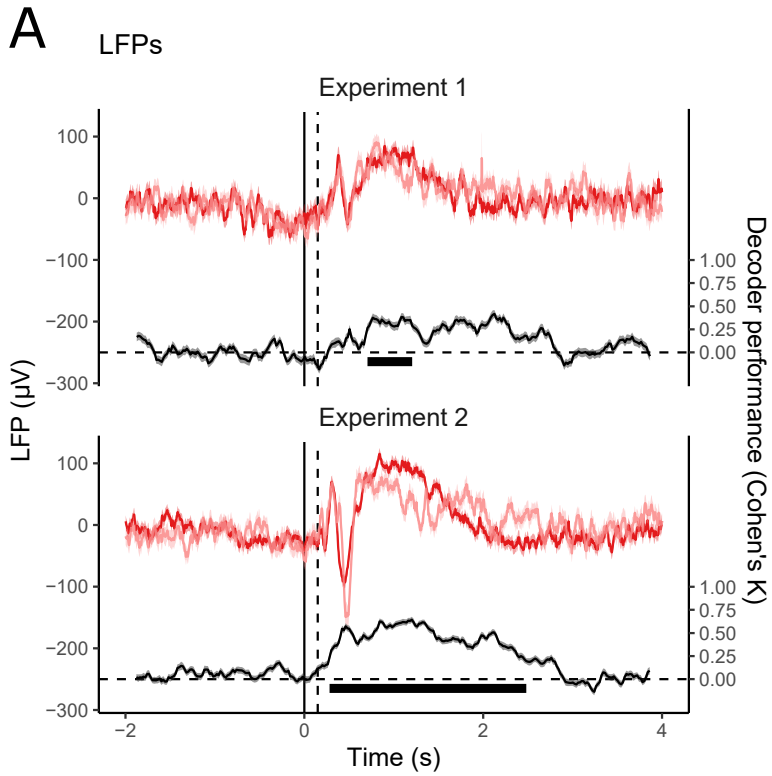
A

Q1, % of "Yes" answers

Visual feedback

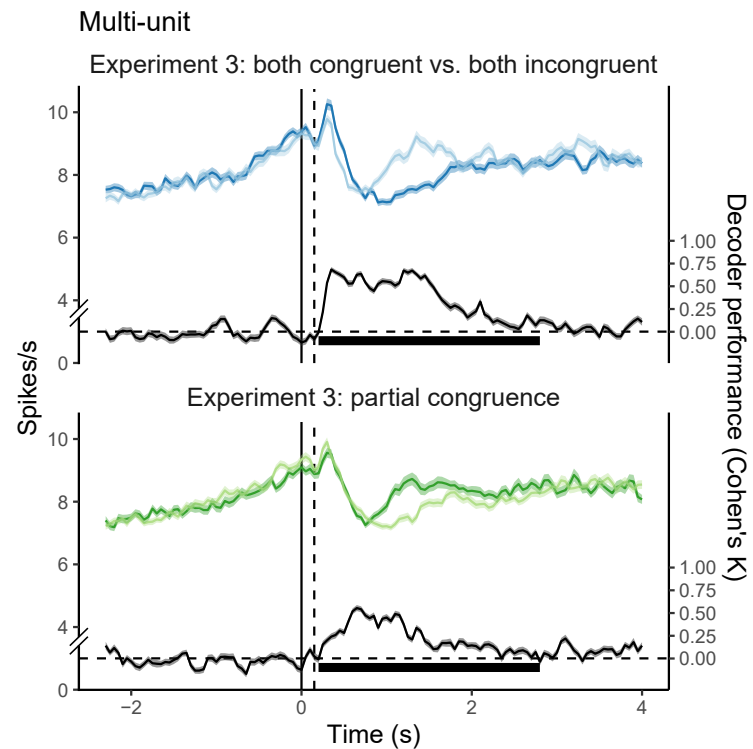
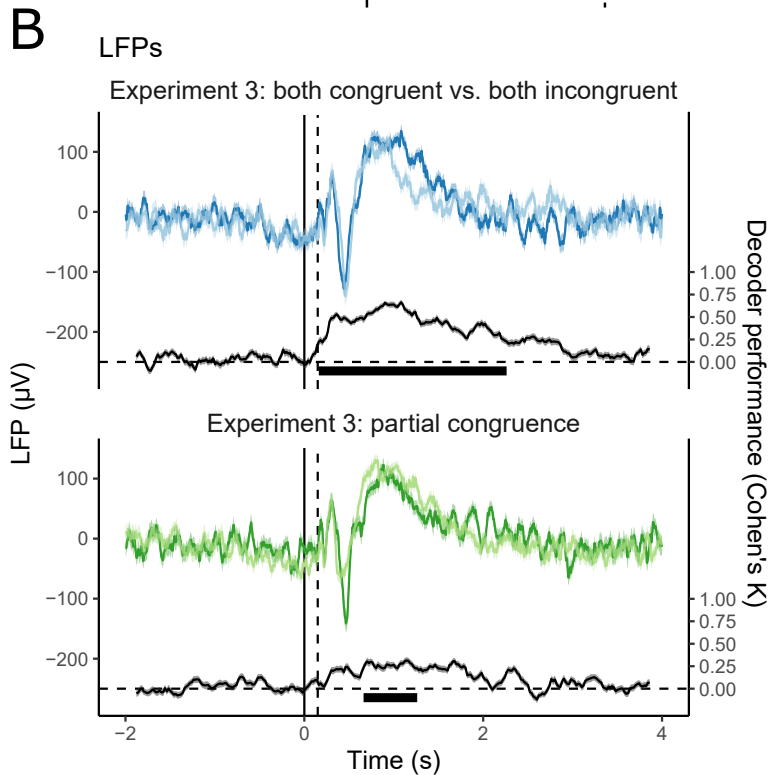
| | | Congruent (+) | None | Incongruent (-) |
|------------------------|-----------------|------------------|------------------|------------------|
| Somatosensory feedback | Congruent (+) | Exp. 3 100 % | Exp. 2 97.4 % | Exp. 3 68.5 % |
| | None | Exp. 1 94 % | | Exp. 1 5.6 % |
| | Incongruent (-) | Exp. 3 52.5 % | Exp. 2 9 % | Exp. 3 7.8 % |

B**C****D**



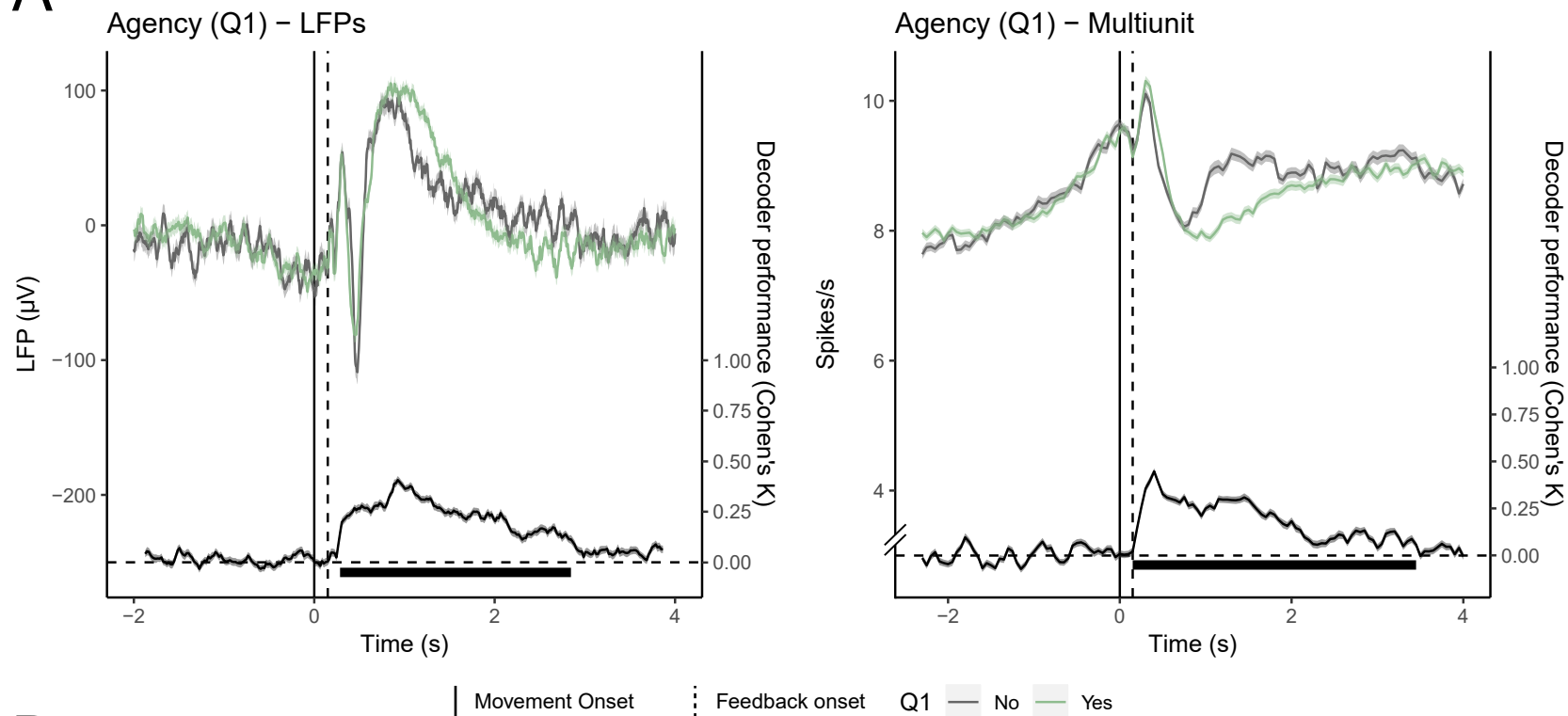
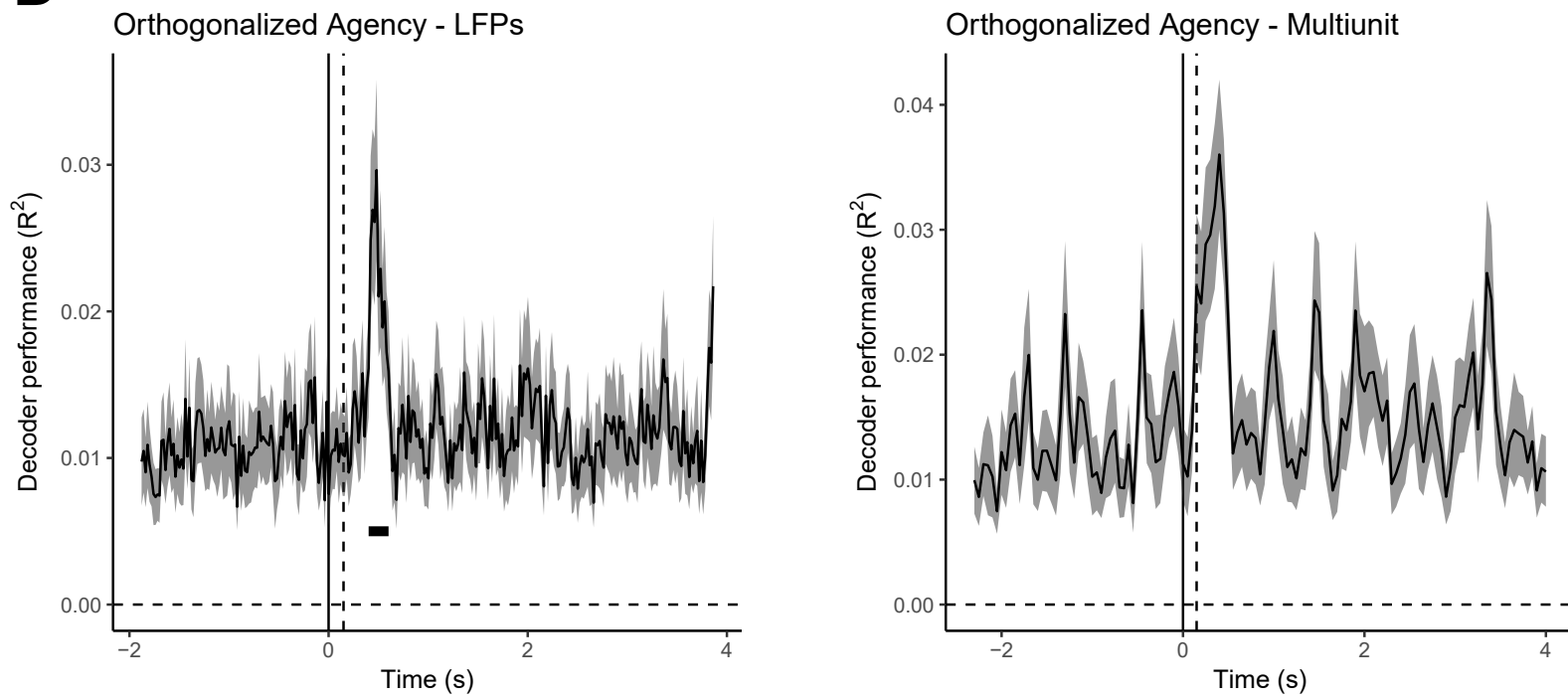
Feedback

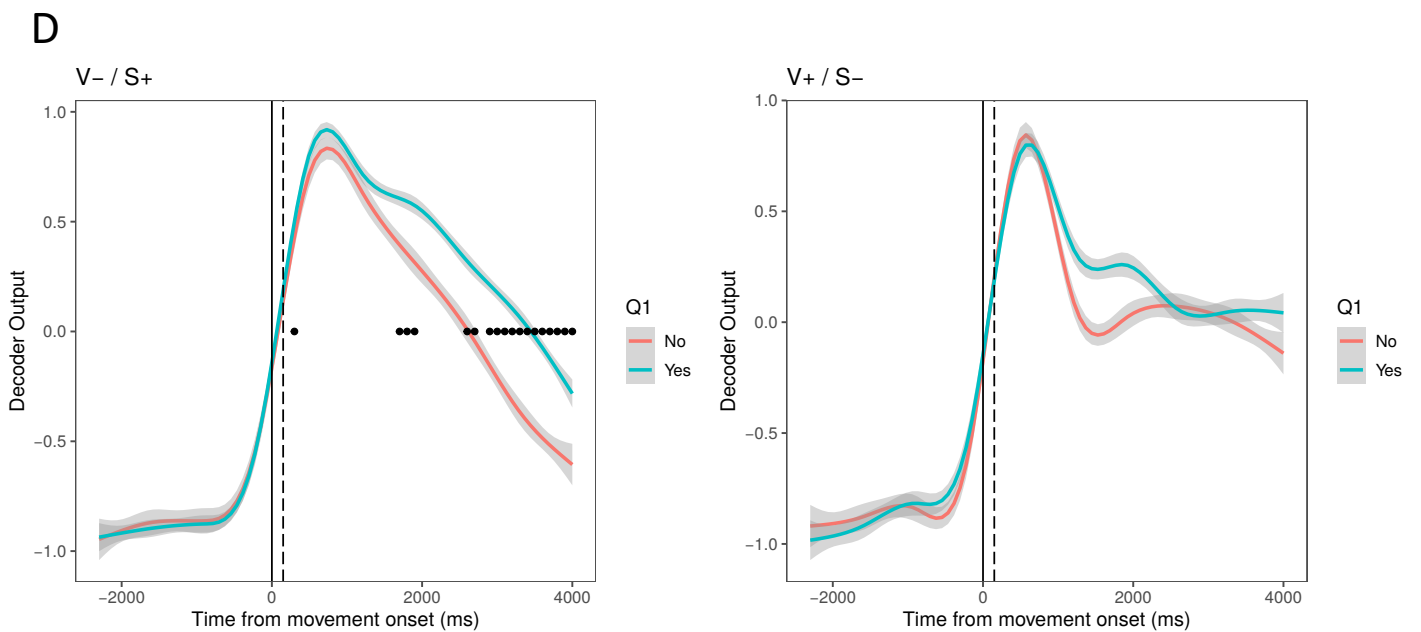
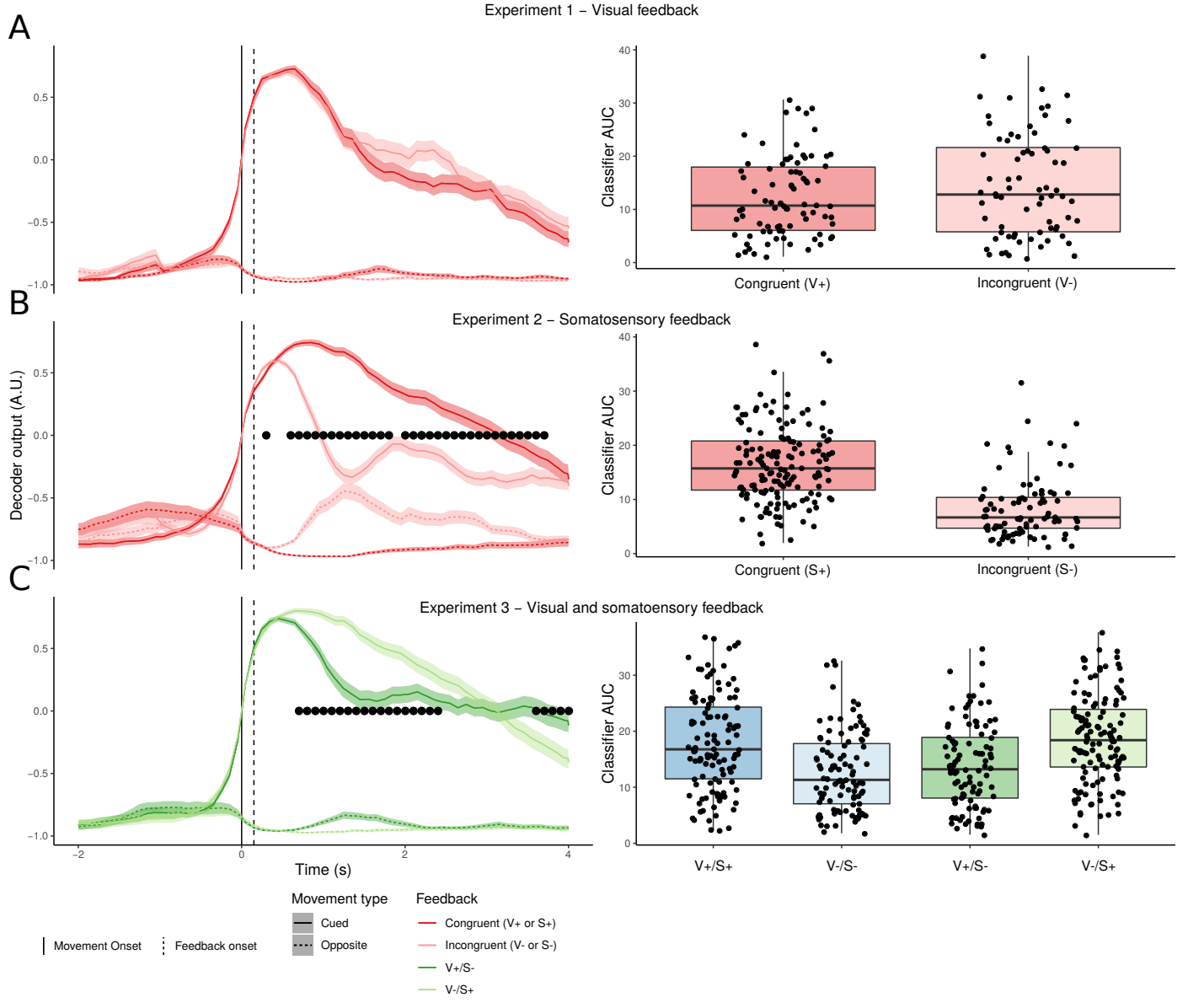
— Congruent (V+ or S+) — Incongruent (V- or S-)

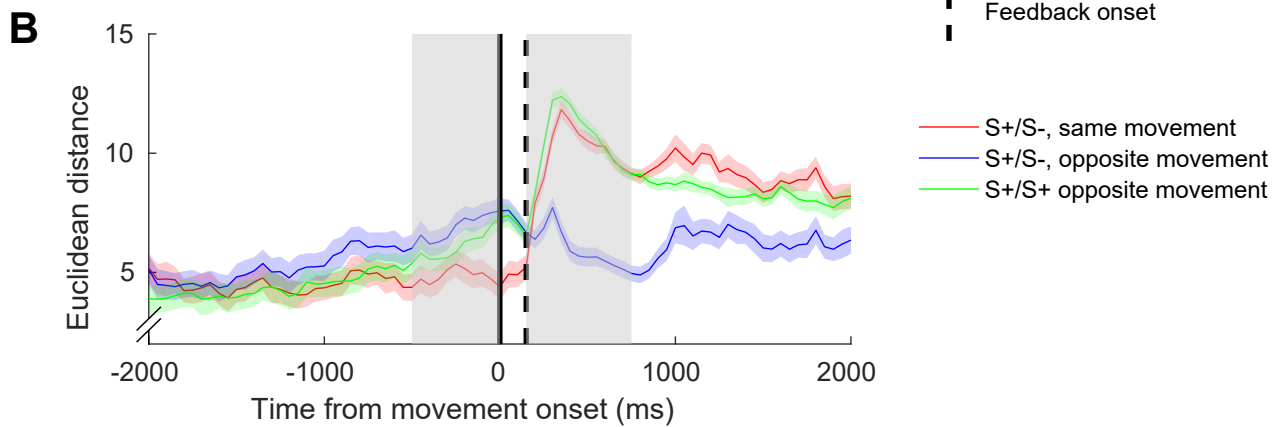
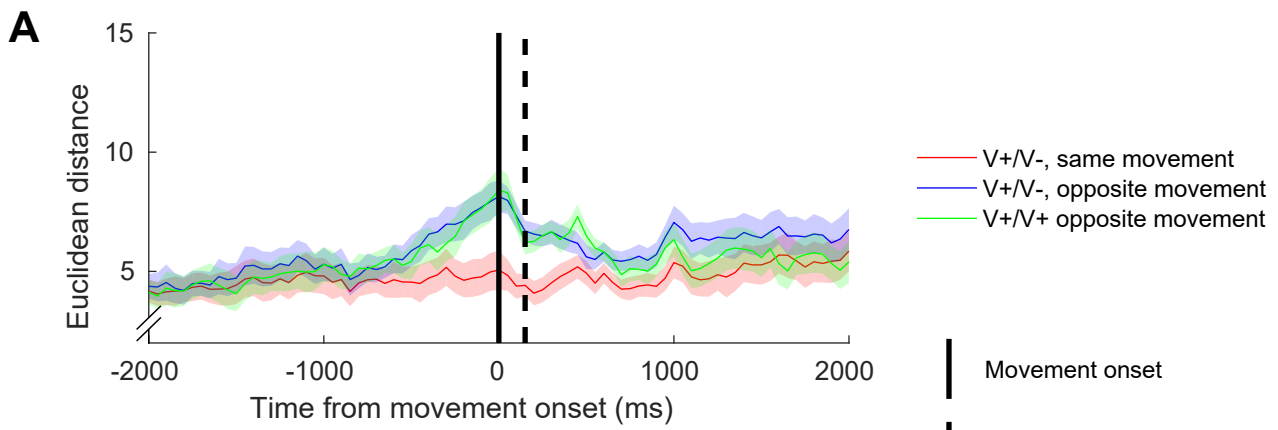


Feedback

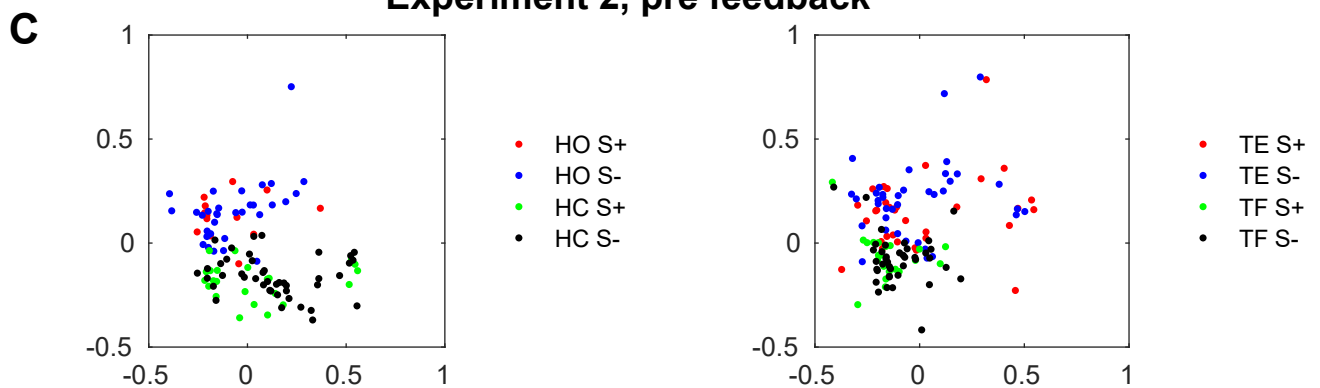
— V+/S+ — V-/S-
— V+/S- — V-/S+

A**B**





Experiment 2, pre feedback



Experiment 2, post feedback

